




Cellular/Molecular

G272V and P301L Mutations Induce Isoform Specific Tau Mislocalization to Dendritic Spines and Synaptic Dysfunctions in Cellular Models of 3R and 4R Tau Frontotemporal Dementia

Ke Yu,^{1,2*}  Katherine R. Yao,^{1,3*}  Miguel A. Aguinaga,^{1,3} Jessica M. Choquette,¹ Chengliang Liu,¹ Yuxin Wang,¹ and  Dezhi Liao¹

¹Department of Neuroscience, University of Minnesota, Minneapolis, Minnesota 55455, ²Department of General Practice, The General Hospital of Western Theater Command, Chengdu 610083, China, and ³College of Biological Sciences, University of Minnesota, St Paul, Minnesota 55108

Tau pathologies are detected in the brains of some of the most common neurodegenerative diseases including Alzheimer's disease (AD), Lewy body dementia (LBD), chronic traumatic encephalopathy (CTE), and frontotemporal dementia (FTD). Tau proteins are expressed in six isoforms with either three or four microtubule-binding repeats (3R tau or 4R tau) due to alternative RNA splicing. AD, LBD, and CTE brains contain pathological deposits of both 3R and 4R tau. FTD patients can exhibit either 4R tau pathologies in most cases or 3R tau pathologies less commonly in Pick's disease, which is a subfamily of FTD. Here, we report the isoform-specific roles of tau in FTD. The P301L mutation, linked to familial 4R tau FTD, induces mislocalization of 4R tau to dendritic spines in primary hippocampal cultures that were prepared from neonatal rat pups of both sexes. Contrastingly, the G272V mutation, linked to familial Pick's disease, induces phosphorylation-dependent mislocalization of 3R tau but not 4R tau proteins to dendritic spines. The overexpression of G272V 3R tau but not 4R tau proteins leads to the reduction of dendritic spine density and suppression of mEPSCs in 5-week-old primary rat hippocampal cultures. The decrease in mEPSC amplitude caused by G272V 3R tau is dynamin-dependent whereas that caused by P301L 4R tau is dynamin-independent, indicating that the two tau isoforms activate different signaling pathways responsible for excitatory synaptic dysfunction. Our 3R and 4R tau studies here will shed new light on diverse mechanisms underlying FTD, AD, LBD, and CTE.

Key words: Alzheimer's disease; AMPA receptors; dendritic spines; dynamin; frontotemporal dementia; tau mislocalization

Significance Statement

Frontotemporal dementia (FTD) is the third most common form of dementia caused by neurodegeneration with diverse clinical presentations. Here, we report distinct cellular mechanisms that may explain some of the similarities and differences between diverse forms of frontotemporal dementia. Tau proteins are composed of six isoforms. We found that although all isoforms can cause neural deficits, each isoform may impair the structures and functions of neurons with different temporal dynamics or through different mechanisms. The mechanistic studies of isoform-specific tau-mediated synaptic impairments reported here will add valuable information to the current molecular and cellular framework, by which diverse tau isoforms cause brain deficits in frontotemporal dementia and other neurodegenerative diseases including Alzheimer's diseases, Lewy body dementia, and chronic traumatic encephalopathy.

Received June 27, 2023; revised May 10, 2024; accepted May 16, 2024.

Author contributions: K.Y. and D.L. designed research; K.Y., K.R.Y., M.A.A., J.M.C., C.L., Y.W., and D.L. performed research; K.Y., J.M.C., C.L., Y.W., and D.L. contributed unpublished reagents/analytic tools; K.Y., K.R.Y., M.A.A., and D.L. analyzed data; K.Y. and D.L. wrote the paper.

We thank Dr. Michael Koob for his technical expertise and thoughtful discussions and our funding sources: NIH Grant Numbers R01 AG075809-01 (D.L.), R61/R33 NS115089 (D.L.), and 9R42AG083665-02A1 (D.L.); USU-UMN DOD Partnership Grant I80VP000437-01 (D.L.), R21-NS084007-01 (D.L.), and

R21-NS096437-01 (D.L.); NSF CMMI 1935834 (D.L.); UMN-Mayo Partnership Grant (D.L.); and Minnesota Higher Education Grant (D.L.).

*K.Y. and K.R.Y. contributed equally to this work.

The authors declare no competing financial interests.

Correspondence should be addressed to Dezhi Liao at liaox020@umn.edu.

<https://doi.org/10.1523/JNEUROSCI.1215-23.2024>

Copyright © 2024 the authors

Introduction

FTD is the third most common form of dementia across all age groups, after Alzheimer's disease (AD) and Lewy body dementia (LBD; Vieira et al., 2013; Bang et al., 2015; Sanford, 2018). The FTD superfamily is now separated into three subfamilies including FTD-tau, FTD-TDP, and FTD-FUS, which contain tau, TDP43, and FUS pathologies, respectively (Kertesz et al., 2003; Cairns et al., 2007; Uchihara and Tsuchiya, 2008; Ling et al., 2013; Bang et al., 2015). Pick's disease is a subgroup of FTD-tau restricted to dementia in patients whose brains contain the specific pathological hallmark of Pick bodies (Kertesz et al., 2003; Cairns et al., 2007; Uchihara and Tsuchiya, 2008).

Tau binds to microtubules through multiple interacting sites within three or four microtubule-binding repeats (Rs), and its microtubule interactions are modulated by amino acid sequences in the adjacent proline-rich region (Butner and Kirschner, 1991; Goode et al., 1997). Due to alternative RNA splicing, tau proteins are expressed in six isoforms with either three or four microtubule-binding repeats (Kosik et al., 1989; Andreadis et al., 1992; Andreadis, 2005; Qian and Liu, 2014; Regan et al., 2017). Among the six isoforms, three tau isoforms possess three microtubule-binding repeats (3R tau), and three isoforms possess four repeats (4R tau). While most neurodegenerative diseases including AD, LBD, and chronic traumatic encephalopathy (CTE) exhibit mixed 3R and 4R tau pathologies (Iseki et al., 2003; Hasegawa et al., 2014; Arena et al., 2020; Dregni et al., 2022), FTD patients often exhibit either exclusively 4R tau pathologies or exclusively 3R tau pathologies (Cairns et al., 2007; Hu et al., 2007; Dickson et al., 2011). The 3R tau FTD is called Pick's disease because its pathological hallmark, Pick body, contains exclusively 3R tau (Cairns et al., 2007; Uchihara and Tsuchiya, 2008).

Genetic mutations in the tau gene on chromosome 17 lead to the familial form of FTD, which is also called frontotemporal dementia with Parkinsonism linked to chromosome 17 (FTDP-17; Yamaoka et al., 1996; Heutink et al., 1997; Wszolek et al., 2006; Ghetti et al., 2015). The P301L and G272V were among the first genetic mutations found to be associated with FTDP-17 (Hutton et al., 1998). The P301L mutation is linked to 4R tau FTDP-17 as the postmortem neural tissues from these patients possess neurofibrillary tangles that are composed of 4R tau (Ghetti et al., 2015). Contrastingly, the G272V mutation is instead associated with 3R tau FTDP-17, which is also called familial Pick's disease (Bronner et al., 2005). Despite the clear pathological difference between 3R and 4R tau FTDP-17, the clinical presentations of these two diseases share many similarities (van Swieten et al., 1999; Hu et al., 2007), suggesting a common mechanism underlying synaptic and cognitive deficits caused by 3R and 4R tau.

Increasing studies suggest that diverse neurodegenerative diseases share common pathological hallmarks and cellular mechanisms (Tracy and Gan, 2018; Teravskis et al., 2020). One common mechanism involves 4R tau mislocalization into dendritic spines (Hoover et al., 2010; Ittner et al., 2010; Miller et al., 2014; Teravskis et al., 2018, 2020; Singh et al., 2019; Braun et al., 2020), which are postsynaptic structures found in most excitatory glutamatergic synapses (Harris and Kater, 1994; Kennedy, 2000). However, how pathological 3R tau proteins affect dendritic spines is still unknown. Here, we introduced the G272V mutation into both 3R and 4R tau proteins and transfected them into primary rat hippocampal cultures. We also tested the P301L mutant 4R tau in the same cellular system.

We found that, unlike P301L, the G272V mutation induces the mislocalization of 3R tau proteins to dendritic spines but not 4R tau proteins. The mislocalization of 3R tau proteins correlates with spine loss and profound synaptic dysfunction. Importantly, the synaptic dysfunction caused by 3R tau is dynamin-dependent, while that by 4R tau is not, indicating that the two tau isoforms activate distinct signaling cascades. The distinct tau mechanisms unraveled here will help us better understand the complex disease mechanisms underlying diverse tauopathies.

Materials and Methods

Animal care and usage. Sprague Dawley timed-pregnancy adult rats were housed in facilities of Research Animal Resources (RAR) at the University of Minnesota after being delivered from Envigo (www.envigo.com). The rats were fed a diet of regular chow before giving birth. Rat pups were killed by decapitation to harvest brain tissues in postnatal day 0 to day 2. All work was conducted in accordance with the American Association for the Accreditation of Laboratory Animal Care and Institutional Animal Care and Use Committee (IACUC) at the University of Minnesota (protocol #1211A23505). We performed all procedures of euthanasia strictly according to the guidelines of the IACUC at the University of Minnesota.

Materials. All common chemical reagents and cell culture supplies were purchased from Sigma-Aldrich, Fisher Scientific, Promega, VWR, and Thermo Fisher Scientific/Invitrogen/Life Technologies unless otherwise indicated.

Plasmids and PCR mutagenesis. All human tau and DsRed constructs were expressed in the pRK5 vector and driven by the cytomegalovirus promoter (Clontech). All human tau proteins were N-terminally fused to enhanced GFP (eGFP), which allows visualization of neurons for live imaging and electrophysiological experiments. The initial template of wild-type, native human tau construct encoded a human 4R tau lacking the transcriptional-variant N-terminal sequences (0N4R). It contained exons 1, 4, 5, 7, 9–13, and 14 and intron 13 (see details in RRID:Addgene_46904). G272V and P301L mutants were created using a stepwise site-directed mutagenesis (QuikChange SDM Kit, Aligent). PCR primers for mutagenesis were 15–22 nucleotides long, centered on mutated nucleotide(s) (Integrated DNA Technologies). The plasmids encoding 3R tau proteins were made by the deletion of the second microtubule-binding repeat (amino acids 280–305) based on previous publications (Kolarova et al., 2012) utilizing a standard PCR protocol. All nucleotide mutations and plasmid construct integrity were confirmed with Sanger sequencing (UMN Genomics Center). Tau sequence numbering was based on the longest functional human isoform: 441-tau (2N4R tau; NCBI reference sequence: NP_005901.2).

Primary hippocampal neuron cultures. Briefly, a 22-mm-diameter glass coverslip (0.09 mm thickness) was fastened with silicone sealant to the bottom of a 35 mm culture dish with a bored hole of 20 mm in diameter and sterilized as we previously described (Lin et al., 2004, 2009) with some modifications. Coverslips were coated with poly-D-lysine. Hippocampi were dissected from decapitated neonatal Sprague Dawley pups from Day 0 to Day 2. Hippocampi from both sexes were pooled together and were enzymatically digested in Earle's balanced salt solution (EBSS) supplemented with 1% glucose and cysteine-activated papain. Digestion was blocked with dilute DNase and trypsin inhibitors (from Sigma-Aldrich), and cells were rinsed in fresh EBSS and plated in plating medium (minimal essential medium with Earle's salts, 10% fetal bovine serum, 5% horse serum, 2 mM glutamine, 10 mM sodium pyruvate, 0.6% glucose, 100 U/ml penicillin, and 100 mg/ml streptomycin) at 1.0×10^6 cells/dish. After 18 h, cell adherence was established, and cells were then grown in a neurobasal medium (NbActiv1; BrainBits). The cultured cells were incubated at 37°C in a 5% CO₂ biological incubator until usage.

Low-efficiency calcium phosphate transfection. At 5–7 d in vitro (DIV), primary rat hippocampal cultures were transfected with bacterial

plasmids encoding the appropriate proteins. DNA plasmid transfection was performed using the standard calcium phosphate precipitation method as we previously described (Lin et al., 2004; Hoover et al., 2010; Miller et al., 2014). Briefly, neurons on 30 mm dishes were cotransfected with human tau constructs and DsRed (2:1 by plasmid DNA mass) for live imaging or transfected with GFP-tagged human tau alone for electrophysiology and immunocytochemistry. To make DNA phosphate precipitates, UltraPure water (Thermo Fisher Scientific), DNA (concentration, 1 mg/ml), calcium chloride (2.5 M), and HEBES solution were mixed at the volumes of 7.5, 6, 1.5, and 15 μ l, respectively, for each dish of cultured neurons. The stock HEBES solution contained the following (in g/L; pH = 7.1): 16 NaCl, 0.71 KCl, 0.38 Na₂HPO₄·7H₂O, 2.7 glucose, and 10 HEPES. The abovementioned mixed solution of precipitated DNA was applied to cells in a 100 μ l solution of glial conditioned medium (neurobasal medium previously conditioned for 14 d on a glial monolayer and reserved) containing 100 μ M APV, an NMDA receptor antagonist, to prevent calcium-induced excitotoxicity. The cells were subsequently incubated at 37°C for 3–4 h to allow cells to take DNAs. Thereafter, cells were taken out and rinsed with the glial conditioned medium. After the medium was replaced again with the neurobasal medium, the cells were put back into the incubator to grow until mature (19 DIV or longer). The low transfection rate of this method (~5%) was an advantage for live imaging and electrophysiological studies because it would mostly exclude direct presynaptic effects due to the very low transfection rate of presynaptic terminals (Teravskis et al., 2018, 2021).

Electrophysiology. Miniature excitatory postsynaptic currents (mEPSCs) were recorded from cultured dissociated rat hippocampal neurons at 19–24 DIV (3-week-old groups) or 30–36 DIV (4–5-week-old groups) with a glass pipette (resistance, ~5 M Ω) at holding potentials of ~65 mV on an Axopatch 200B amplifier (output gain, 1; filtered at 1 kHz) as we previously described (Hoover et al., 2010; Teravskis et al., 2021). Tau proteins were GFP-tagged, allowing whole-cell recording of the identified neuron that expresses appropriate tau variants. Input and series resistances were assessed and found to have no significant difference before and after recording time (5–20 min). Sweeps of synaptic responses were sampled continuously for ~30 min (pClamp, v10, RRID:SCR_011323). Neurons were bathed in an oxygenated artificial cerebral spinal fluid (ACSF; gassed with 5% CO₂ and 95% O₂) at room temperature (~23°C) with 100 μ M APV (NMDA receptor antagonist), 1 μ M TTX (sodium channel blocker), and 100 μ M picrotoxin (GABA_A receptor antagonist). ACSF contained the following (in mM): 119 NaCl, 2.5 KCl, 5.0 CaCl₂, 2.5 MgCl₂, 26.2 NaHCO₃, 1 NaH₂PO₄, and 11 D-glucose. The internal solution of the glass pipettes contained the following (in mM): 100 cesium gluconate, 0.2 EGTA, 0.5 MgCl₂, 2 ATP, 0.3 GTP, and 40 HEPES. The pH of the internal solution was normalized to 7.2 with cesium hydroxide and diluted to a trace osmotic deficit in comparison with ACSF (~300 mOsm). All analyses of recordings were performed manually (Mini Analysis Program, v6.0.7, RRID:SCR_002184 from Synaptosoft or Clampfit from Molecular Devices). Minimum analysis parameters were set at greater than 1 min stable recording time and event amplitude greater than 3 pA. An mEPSC event was identified by distinct fast-rising depolarization and slow-decaying repolarization. Each event was a synaptic response mediated by α -amino-3-hydroxy-5-methyl-4-isoxazolepropionic acid receptors (AMPA receptors) as NMDA and GABA_A receptors were blocked by APV and picrotoxin. Combined individual events were used to form relative cumulative frequency curves, while the means of all events from individual recordings were treated as single samples for further statistical analysis. Example traces were exported from Mini Analysis or Clampfit. They were live traced, simplified, and united in vector editing software (Adobe Illustrator CS5, v15, RRID:SCR_010279 or Microsoft PowerPoint).

Image analysis of live neuronal cultures. Transfected cells were continually bathed in neurobasal media and were passively perfused with medical-grade 95% O₂–5% CO₂ (Hoover et al., 2010; Teravskis et al., 2021). Micrographs were taken on a Nikon epifluorescent inverted microscope with a 60 \times oil lens with a computerized focus motor when

neurons were 3 or 5 weeks old. All digital images were processed using microscopic imaging software (MetaMorph Microscopy Automation and Image Analysis Software, v7.1, RRID:SCR_002368). Images were taken as 15-plane Z-stacks at 0.5 μ m increments, processed by deconvolution to the nearest planes, and averaged against other stacked images. A dendritic spine was defined as having an expanded head diameter, greater than 50% larger in diameter than the neck. The number of spines labeled by DsRed per neuron was counted and normalized to a 100 μ m length of dendritic shaft.

Pharmacology. GSK3 β and CDK5 inhibitors, Roscovitine and CHIR99021, respectively, were purchased from Sigma-Aldrich and were diluted in DMSO to 1,000 \times concentration aliquots for an ultimate concentration in neurobasal medium of 0.5 μ M. As we previously reported, the complete prevention of tau mislocalization to dendritic spines requires the blockade of both kinases (Teravskis et al., 2021). Therefore, primary cultured rat hippocampal neurons were concurrently treated with both drugs when the neurons were 5 weeks old unless stated otherwise in the main text. Treated cells were incubated for 24 h prior to imaging or electrophysiological experiments. Cell death was visually assessed under differential interference contrast (DIC) for decreased cell density, lost soma adhesion, and gross qualitative neurite retraction. If evidence of cell death was observed under DIC, cells were fixed in 4% sucrose and 4% paraformaldehyde in phosphate-buffered saline (PBS) and stained with 300 nM 4',6-diamidino-2-phenylindole (DAPI) in PBS. DAPI-stained cells were analyzed under fluorescent microscopy for nuclear pyknosis and karyorrhexis. As reported previously (Braun et al., 2020; Teravskis et al., 2021), no overt neuronal apoptosis was detected when neurons were concurrently treated with 0.5 μ M Roscovitine and 0.5 μ M CHIR99021 or at lower dosages. Therefore, these doses were used for live imaging (Fig. 5), electrophysiological experiments (Fig. 6), and Pick body detection experiments (Fig. 7) to test the involvement of GSK3 β and CDK5 kinases in tau-mediated synaptic impairments and the formation of Pick bodies.

Dynasore (from www.abcam.com; #ab120192) is a cell-permeable, noncompetitive inhibitor of dynamin 1, dynamin 2, and Drp1 with IC50 of approximately 15 μ M in HeLa cells and blocks clathrin-dependent endocytosis within 30 min (Macia et al., 2006). Accordingly, we prepared an initial stock solution of dynasore in DMSO at a concentration of 100 mM and further diluted it with 100% ethanol by threefold (adding 100 μ l of ethanol to 50 μ l of the initial stock solution) to obtain a working solution of dynasore (33.3 mM). In 1–2 d before electrophysiological recording, we added 1 μ l of the working solution to each dish of primary hippocampal cultures with ~2.25 ml of media, reaching a final concentration of ~15 μ M, which was comparable to the IC50 in HeLa cells (Macia et al., 2006). We did not apply dynasore at a higher dose to avoid neurotoxicity as our treatment time was much longer than that in the prior study (Macia et al., 2006).

Immunocytochemistry of tau and DAPI staining of the nucleus. For the assessment of asymmetric aggregation of tau around the nucleus, 5-week-old neurons were fixed and permeabilized as previously described (Lin et al., 2009). Cultured neurons were fixed and permeabilized with 4% paraformaldehyde + 4% sucrose (room temperature, 30 min), and 0.2% Triton X-100 (room temperature, 20 min) was applied successively as previously described (Lin et al., 2009). The cells on the glass bottom of a 35 mm culture dish were washed with PBS three times and incubated with 2.5 ml of DAPI at a concentration of 300 nM in PBS for 5 min. The cells were washed with PBS again three times and then blocked with 10% normal goat serum (NGS) at room temperature for 20 min (Jackson ImmunoResearch, catalog #005-000-121). The culture dishes were immediately mounted on an inverted fluorescence microscope, and images of both GFP and DAPI were taken in the same neuron expressing GFP-tagged tau proteins through the green and blue fluorescence channels, respectively. The asymmetric aggregation of tau next to the nucleus was quantified as described in the main text.

For the immunostaining of phosphorylated tau proteins, neurons were fixed and permeabilized as described above. The cultures were

washed with PBS three times and blocked with 10% NGS at room temperature for 20 min (Jackson ImmunoResearch, catalog #005-000-121). Neurons were coincubated with a primary mouse monoclonal AT8 anti-phospho-tau antibody (purified; Thermo Fisher Scientific, catalog #MN1020, RRID:AB_223648; targeting phospho-S202 and phospho-T205 residues; diluted at 1:200 in 10% NGS; Goedert et al., 1995) and a primary rabbit polyclonal anti-GFP antibody (to compensate for decreased eGFP signal due to fixation; Thermo Fisher Scientific, catalog #A-11122, RRID:AB_221569; diluted at 1:200 in 10% NGS) at 4°C overnight. The neurons were washed with PBS three times and subsequently incubated with two secondary antibodies from Jackson ImmunoResearch (goat rhodamine anti-mouse, catalog #111-025-003, RRID:AB_2337926, and goat FITC anti-rabbit, catalog #111-095-003, RRID:AB_2337972) at a dilution of 1:200 in 10% NGS for 1 h at room temperature. An 18 mm glass coverslip was mounted on the stained cultures, which were examined with a Nikon microscope. Fluorescence intensity was derived from peak pixel intensity taken at the middle of a dendrite branch (named as “Fneuron”) and normalized by pixel intensity of adjacent background fluorescence (named as “Fbackground”) using the MetaMorph software. The normalization was performed using the following equation: $\text{normalized } F = (\text{Fneuron} - \text{Fbackground}) / \text{Fbackground}$. The ratio of normalized fluorescence intensity of AT8 (F-AT8; the red channel) versus normalized fluorescence intensity of total GFP-tagged tau (F-GFP; the green channel) was calculated in each examined neuron. The means of this ratio were compared between individual groups with the two-way ANOVA using the Origin software (Fig. 8).

Statistics and figure design. All statistics were performed in biological statistical analysis software (GraphPad Prism, v6; or Origin). We utilized one- and two-way ANOVA for univariate and multivariate analysis, respectively. If ANOVA revealed significant variance between all groups, post hoc analysis was performed using Bonferroni’s analysis adjusted for multiple groups. Univariate cumulative frequency distributions were compared using the unmodified Kolmogorov–Smirnov goodness-of-fit test (K–S test). Single comparisons were analyzed using Student’s *t* test. For all analyses, statistical significance was set at $\alpha = 0.05$. Data representations are described in the respective figure legends. In the histograms in all figures, the height and error bar represent the mean and standard error, respectively. Figures were designed and created using Adobe Photoshop CS5 (v12, RRID:SCR_014199) to create TIFF and PDF images.

Results

G272V mutation induces mislocalization of 3R tau but not 4R tau to dendritic spines in relatively young cultured hippocampal neurons (3 weeks in vitro)

Phosphorylation-dependent tau mislocalization to dendritic spines has been shown in cellular and animal models of multiple neurodegenerative diseases including AD, FTDP-17, LBD, and CTE (Singh et al., 2019; Braun et al., 2020; Teravskis et al., 2020). The G272V mutation in the tau gene is linked to familial Pick’s disease, which is a 3R tau FTD (van Swieten et al., 1999; Bronner et al., 2005). To test whether tau mislocalization to dendritic spines is a shared cellular mechanism for both 3R and 4R tau FTD, we first made plasmids encoding 3R WT tau by truncating the secondary microtubule-binding repeat through PCR mutagenesis (see Materials and Methods). The G272V mutant 3R tau construct was then made by further point mutagenesis (Fig. 1A). A G272V mutant 4R tau was also made by point mutagenesis for comparison (Fig. 1A). The 4R WT tau and P301L mutant 4R tau were also included for appropriate comparisons (Fig. 1A) and have been made and characterized in our previous studies (Hoover et al., 2010).

We prepared primary hippocampal neurons from neonatal rat pups of both sexes from Day 0 to Day 2 after birth and utilized

the standard calcium phosphate precipitation method to introduce DNAs to cultured neurons (see Materials and Methods). The advantage of this protocol is that presynaptic terminals are rarely transfected, and the observed changes would mostly result from the postsynaptic presence of tau (Teravskis et al., 2018, 2021). We cotransfected the cultured neurons with a plasmid encoding DsRed and another plasmid encoding GFP-tagged WT 3R tau, WT 4R tau, P301L mutant 4R tau, G272V mutant 3R tau, or G272V mutant 4R tau proteins using a method we previously reported (Fig. 1B; see Materials and Methods; Hoover et al., 2010; Teravskis et al., 2018). The neurons were transfected with the plasmids after 5–7 d in vitro and photographed with live imaging at 3 weeks in vitro, resulting in an expression duration of 2 weeks. We found that, like WT 4R tau, WT 3R tau was mostly located in the shafts of dendrites and rarely present in dendritic spines (Fig. 1B, first and second rows). Consistent with previous studies (Hoover et al., 2010), P301L mutant 4R tau proteins were missorted to dendritic spines (Fig. 1B, third row). Interestingly, the G272V mutation induced the mislocalization of 3R tau (Fig. 1B, fourth row) but not 4R tau (Fig. 1B, 5th row) to dendritic spines, supporting a role for 3R tau mislocalization in the pathobiology of familial Pick’s disease. Comparing WT 3R tau, the expression of G272V mutant 3R tau significantly increased the proportion of dendritic spines containing GFP-labelled tau versus the total number of spines labeled by DsRed from 18.4 to 76.4% (Fig. 1C; ANOVA, $F = 205.9$; Bonferroni’s after test: $p < 0.001$), supporting 3R tau mislocalization. In contrast, comparing wild-type 4R tau, the expression of G272V mutant 4R tau did not significantly increase the proportion of dendritic spines containing GFP-labeled tau (Fig. 1C; from 14.4 to 16.9%; ANOVA, $F = 205.9$; Bonferroni’s after test: $p > 0.05$), suggesting that 4R tau is not mislocalized. The expression of all forms of tau constructs tested did not significantly change the density of dendritic spines (number of spines/100 μm dendritic length) at the age of 3 weeks in vitro (Fig. 1D; ANOVA, $F = 0.5$; $p > 0.05$ for all means). These results suggest that tau mislocalization to dendritic spines is likely a common mechanism underlying synaptic deficits caused by the pathological conditions in both 3R and 4R tau FTD.

G272V mutation induces no significant changes in excitatory synaptic responses in relatively young cultured hippocampal neurons (3 weeks in vitro)

Our previous studies in multiple tauopathy models have shown that 4R tau mislocalization to dendritic spines is associated with postsynaptic deficits in excitatory synaptic responses and memory tests (Hoover et al., 2010). To investigate how the missorted 3R tau affects synaptic functions in our cellular model of 3R tau FTD, we recorded miniature excitatory postsynaptic currents (mEPSCs) on cultured rat hippocampal neurons at 19–24 d in vitro (DIV) from four groups (untransfected neurons, neurons expressing WT 3R tau, G272V 3R tau, and G272V 4R tau; Fig. 2A). Surprisingly, we found that the expression of either G272V mutant 3R or 4R tau proteins did not significantly change the amplitude (Fig. 2B,C) or the frequency (Fig. 2D,E) of mEPSCs. The expression of G272V mutant 3R or 4R tau proteins did not significantly shift the cumulative frequency curves of mEPSC amplitudes to the left (Fig. 2B), and there is no significant difference between the means of mEPSC amplitudes in the four groups (Fig. 2C; ANOVA, $F = 0.4$, $p > 0.05$ for all means). Similarly, the expression of G272V mutant 3R or 4R tau proteins did not significantly shift the cumulative frequency curves of mEPSC interevent intervals to the right (Fig. 2D), and there is

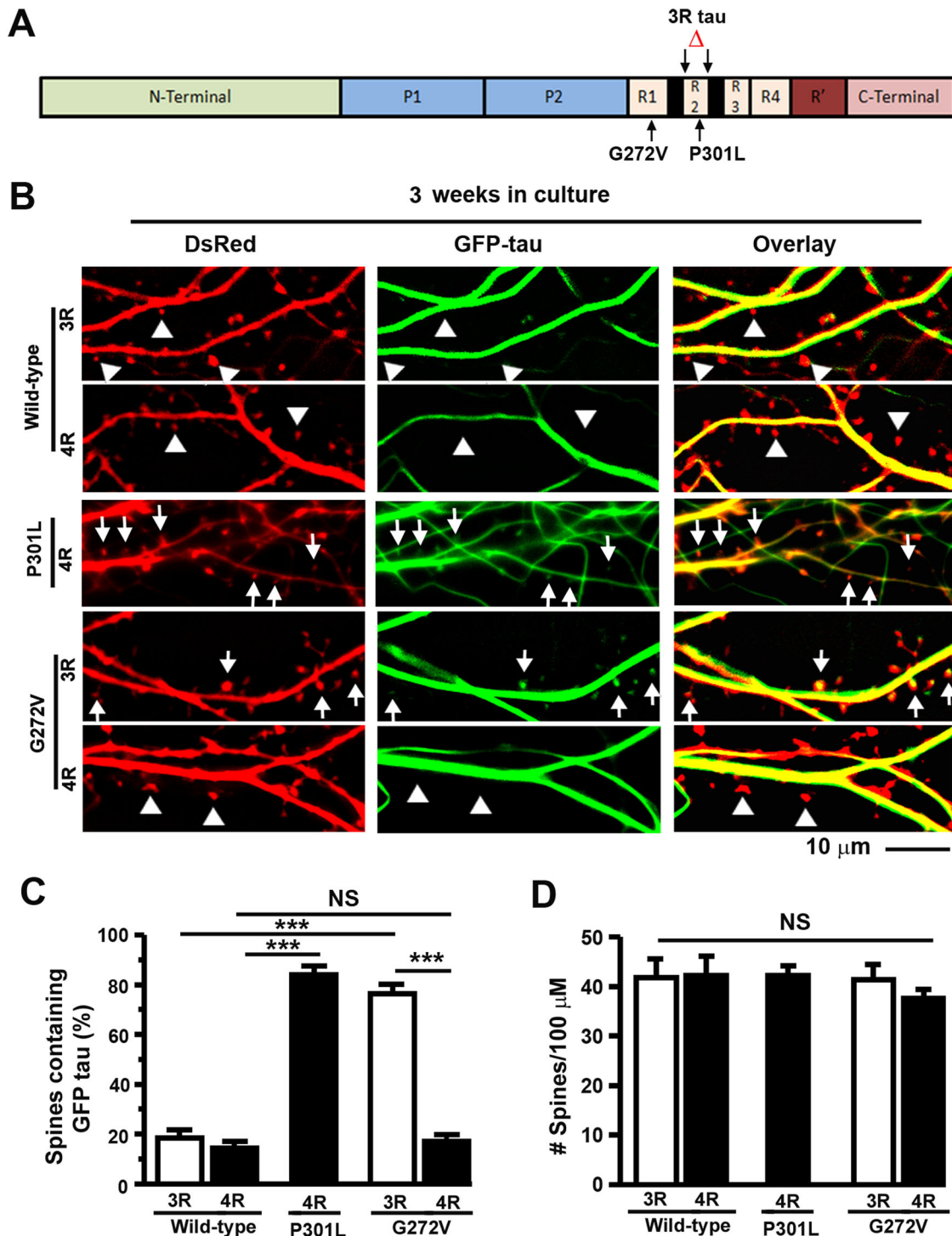


Figure 1. Isoform-specific tau mislocalization to dendritic spines induced by G272V and P301L mutations. **A**, A diagram showing the location of G272V and P301L mutations in tau proteins. The second microtubule-binding repeat (R2) was deleted in all our 3R tau constructs (denoted by the Δ symbol). Note that P301L mutation only exists in 4R tau as it is located in the R2 region (Wszolek et al., 2006; Ghetti et al., 2015). **B**, Representative images of 3-week-old cultured rat hippocampal neurons coexpressing DsRed and various GFP-tagged tau proteins (from top to bottom: wild-type 3R, wild-type 4R, P301L 4R, G272V 3R and G272V 4R tau proteins). The arrows denote dendritic spines that contain tau proteins, and the triangles denote dendritic spines devoid of tau. **C**, Comparisons between the proportions of dendritic spines that contained tau versus the total number of DsRed-labeled spines in dendrites from the above groups ($n = 7$ neurons in each group). ANOVA, NS (not significant), $p > 0.05$; ***, $p < 0.001$. **D**, Comparisons between the densities of dendritic spines (number of spines per 100 μ m length of dendrites) of the above groups. ANOVA, NS (not significant), $p > 0.05$; mean \pm standard error.

no significant difference between the means of mEPSC frequencies in the four groups (Fig. 2E; ANOVA, $F = 0.1$, $p > 0.05$ for all means). These effects together suggest that, although 3R tau is missorted to dendritic spines in 3-week-old cultures, the

missorted 3R tau has not yet impaired the structures and functions of dendritic spines at this relatively young age. These results are clearly different from the effects of missorted 4R tau, which impairs synaptic functions as early as 3 weeks in vitro, as shown

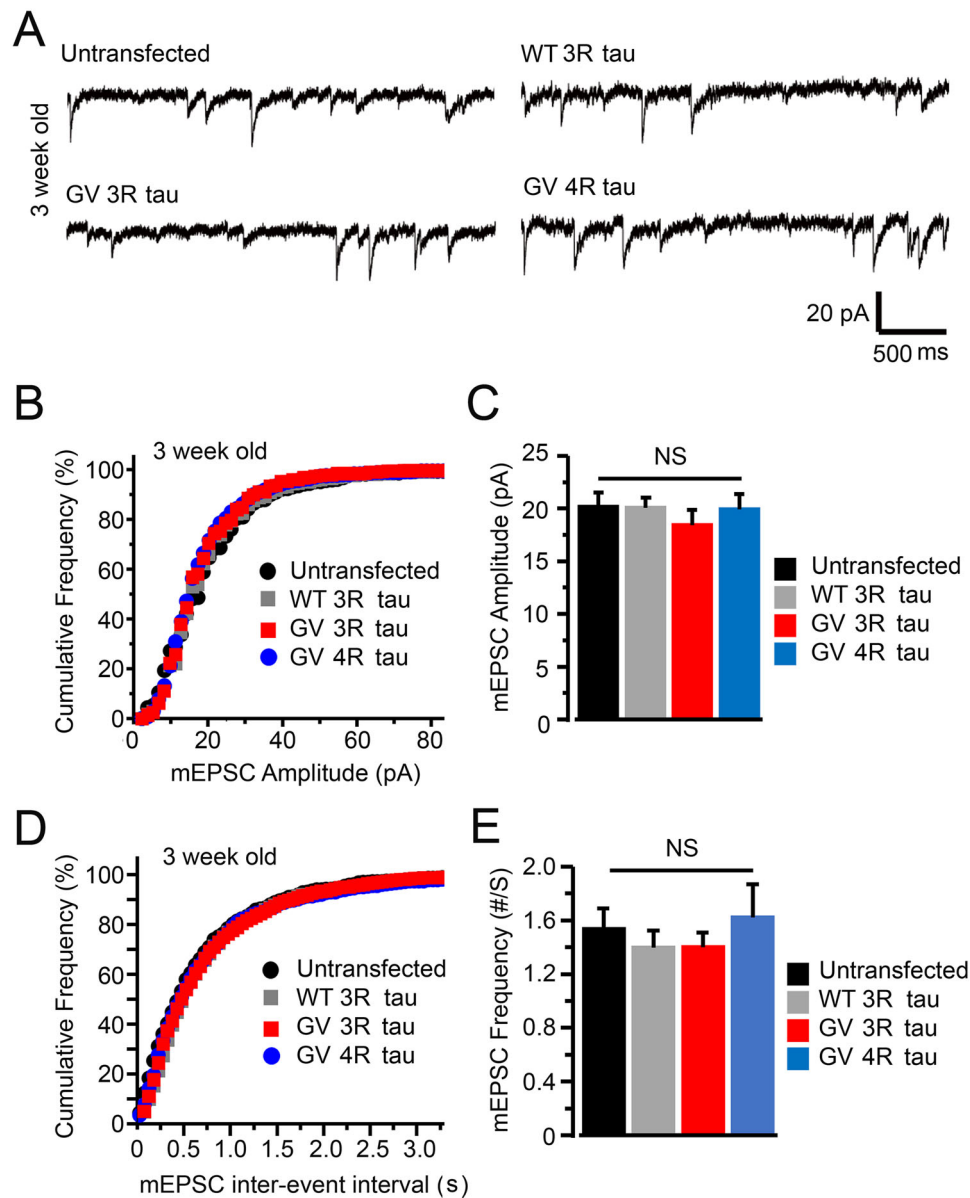


Figure 2. Expression of G272V 3R or 4R tau proteins does not impair synaptic function in 3-week-old neurons. **A**, Representative traces of mEPSCs recorded from untransfected neurons as well as neurons expressing GFP-tagged WT 3R tau, G272V 3R tau, and G272V 4R tau proteins. G272V is abbreviated as “GV” in the labeling. **B**, **C**, Cumulative frequency curves (**B**) and means (**C**) of mEPSC amplitudes in neurons of the above 4 groups ($n = 10$ neurons in each group). **D**, **E**, Cumulative frequency curves of interevent intervals (**D**) and means of mEPSC frequencies (**E**) in the above four groups. $K-S$ tests were used in **B** and **D**. ANOVA tests were used in **C** and **E**. NS (no significant), $p > 0.05$; mean \pm standard error.

in our previous publications (Hoover et al., 2010; Miller et al., 2014; Teravskis et al., 2021).

The expression of G272V mutant tau but not P301L mutant tau induces loss of dendritic spines in old cultured hippocampal neurons (5 weeks in vitro)

As described above, it is puzzling that G272V 3R tau does not impair synaptic function despite being missorted to dendritic spines. In a previous clinical comparative study of behavioral FTD, patients with 4R tauopathies progressed faster and had shorter disease duration than patients with 3R tauopathy (Hu et al., 2007). Therefore, we suspect that, like in human patients, it will also take a longer time for pathogenic 3R tau to impair synaptic structures and function after being missorted to dendritic spines. It has also been known for decades that loss of synapses is the major correlative factor of cognitive impairment in AD

patients (Hamos et al., 1989; Terry et al., 1991; Lippa et al., 1992). This change has also been reported in Pick’s disease cases (Lippa, 2004). Therefore, we tested whether G272V mutant tau leads to loss of dendritic spines in cultures at an older age of 5 weeks in vitro (33–36 d in vitro; Fig. 3). We prepared primary hippocampal neurons from neonatal rat pups in Day 0 to Day 2 after birth and cotransfect the cultured neurons with a plasmid encoding DsRed and another plasmid encoding GFP-tagged WT 3R tau, WT 4R tau, P301L mutant 4R tau, G272V mutant 3R tau, or G272V mutant 4R tau proteins (Fig. 3A). Like in younger cultures (3 weeks in vitro; Fig. 1), WT 3R and 4R tau proteins were mostly located in the shafts of dendrites and rarely present in dendritic spines in neurons as old as 5 weeks in vitro (Fig. 3A,B). Like 3-week-old cultures, P301L mutant 4R tau proteins were also missorted to dendritic spines in 5-week-old cultures (Fig. 3A,B). Again like 3-week-old cultures, the G272V mutation

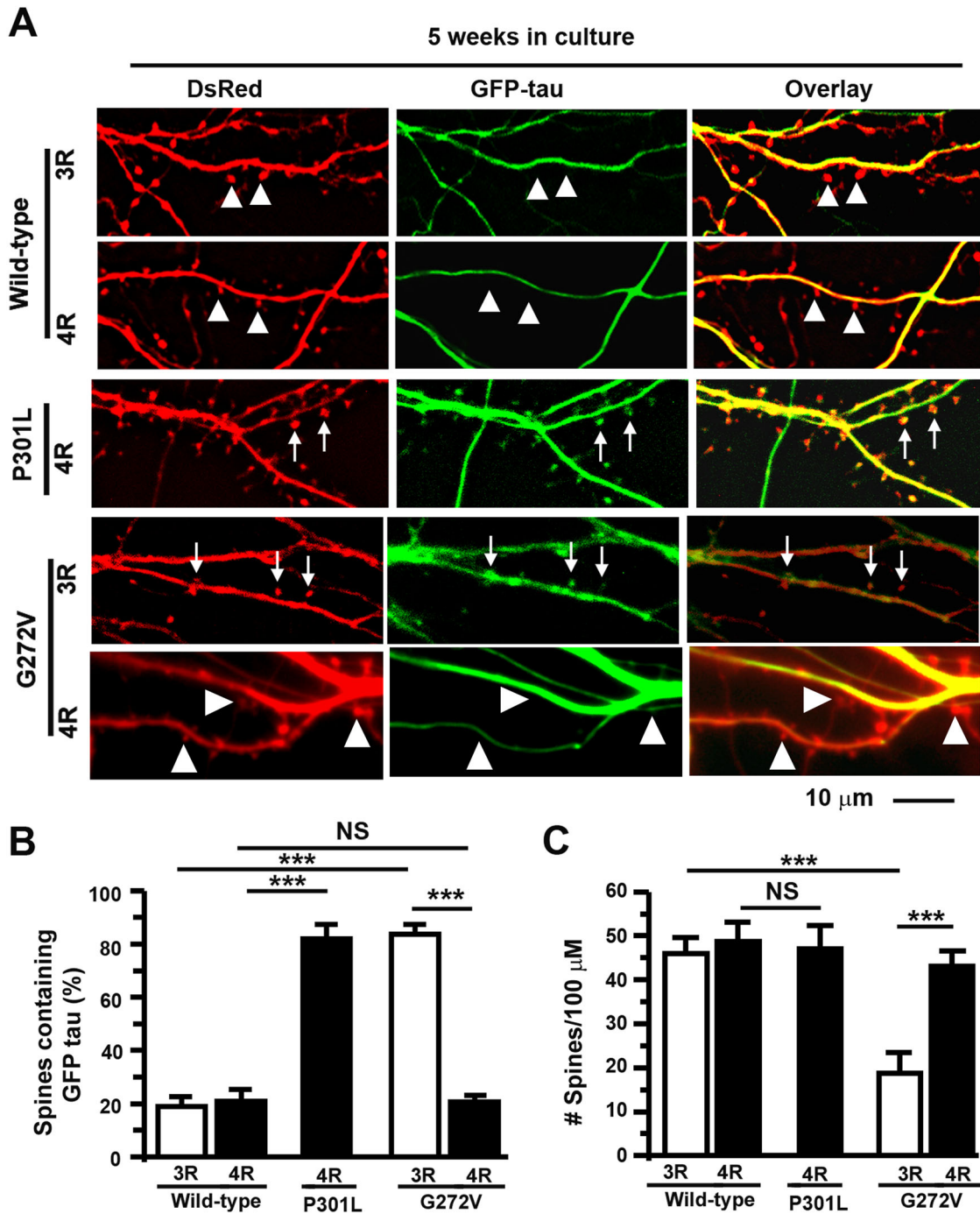


Figure 3. Expression of G272V 3R tau but not 4R tau induces loss of dendritic spines in older primary rat hippocampal cultures (5-week-old). **A**, Representative images of 5-week-old cultured rat hippocampal neurons coexpressing DsRed and various GFP-tagged tau proteins (from top to bottom: wild-type 3R, wild-type 4R, P301L 4R, G272V 3R and G272V 4R tau proteins). The arrows denote dendritic spines that contain tau proteins, and the triangles denote dendritic spines devoid of tau. **B**, Comparisons between the proportions of dendritic spines that contained tau versus the total number of DsRed-labelled spines in dendrites from the above groups ($n = 8$ neurons in each group). ANOVA, ***, $p < 0.001$. **C**, Comparisons between the densities of dendritic spines (number of spines per 100 μm length of dendrites) of the above groups. $n = 7$ neurons in each group, ANOVA, ***, $p < 0.001$; mean \pm standard error.

induced the mislocalization of 3R tau (4th row in Fig. 3A) but not 4R tau (5th row in Fig. 3B) to dendritic spines in 5-week-old cultures, further supporting a role of 3R tau mislocalization in the pathobiology of Pick’s disease. Compared with wild-type 3R tau, the expression of G272V mutant 3R tau significantly increased the proportion of dendritic spines containing GFP-labelled tau versus the total number of spines labeled by DsRed from 18.8 to 83.7% (Fig. 3B; ANOVA, $F = 78.9$;

Bonferroni’s after test: $p < 0.001$). Compared with wild-type 4R tau, the expression of G272V mutant 4R tau did not significantly increase the proportion of dendritic spines containing GFP-labelled tau (Fig. 3B; from 20.8 to 20.7%; ANOVA, $F = 78.9$; Bonferroni’s after test: $p > 0.05$). However, unlike in younger 3-week-old cultures, compared with 3R wild-type tau, the expression of G272V mutant 3R tau significantly decreased the density of dendritic spines from 46.1 to 18.7 spines per

100 μm dendritic length in 5-week-old cultures (Fig. 3C; ANOVA, $F=8.4$; Bonferroni's after test: $p < 0.001$), indicating that the mutant 3R tau can cause loss of dendritic spines. In contrast, compared with wild-type 4R tau, the expression of either P301L or G272V mutant 4R tau proteins did not significantly alter spine density (Fig. 3C; ANOVA, $F=8.4$; Bonferroni's after test: $p > 0.05$ for both proteins). These results indicate that, although tau mislocalization to dendritic spines is a common mechanism for both 3R and 4R tau proteins, only G272V 3R tau affects the structures of dendritic spines after being missorted at least during the experimental period of 5 weeks. This suggests that after being missorted, 3R and 4R tau proteins likely impair the structures of dendritic spines through a different mechanism and/or at a different temporal scale.

The expression of G272V mutant 3R tau protein impairs AMPAR-mediated synaptic responses in old cultured hippocampal neurons (5 weeks in vitro)

To compare the functional roles of 3R tau with 4R tau proteins in older cultures, we have recorded miniature excitatory postsynaptic currents (mEPSCs) in 5-week-old cultured rat hippocampal neurons (33–36 DIV) from four groups (untransfected neurons, neurons expressing wild-type 3R tau, G272V 3R tau, and G272V 4R tau; Fig. 4A). Unlike younger 3-week-old cultures, we found that the expression of G272V mutant 3R tau proteins but not 4R tau proteins overtly decreased the size and occurrence frequency of mEPSC responses (Fig. 4A). The expression of G272V mutant 3R tau proteins but not 4R tau proteins significantly shifted the cumulative frequency curve of mEPSC

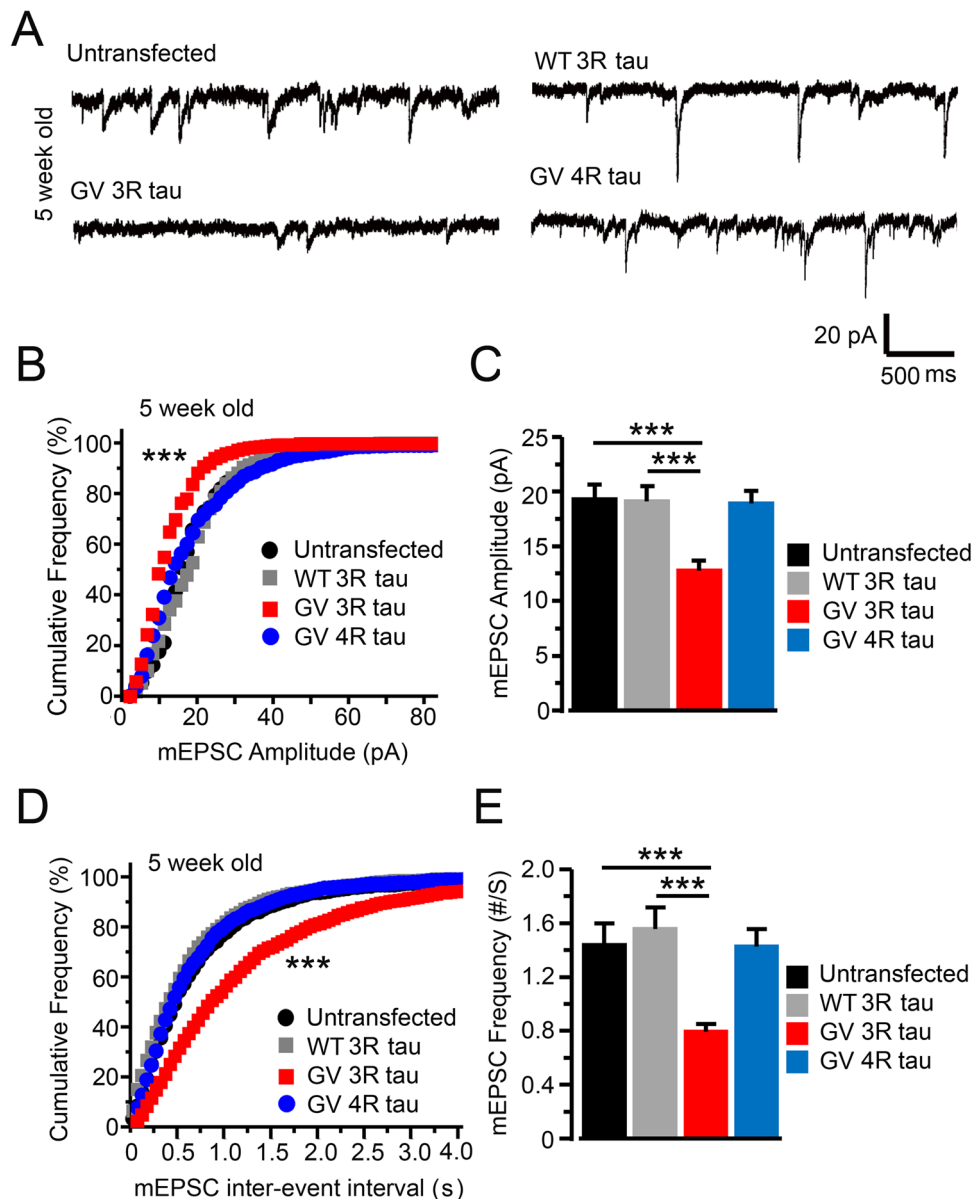


Figure 4. Expression of G272V 3R but not 4R tau proteins impaired synaptic function in older primary rat hippocampal cultures (5-week-old). **A**, Representative traces of mEPSCs recorded from untransfected neurons as well as neurons expressing GFP-tagged WT 3R tau, G272V 3R tau, and G272V 4R tau proteins. G272V is abbreviated as "GV" in the labeling. **B**, **C**, Cumulative frequency curves (**B**) and means (**C**) of mEPSC amplitudes in neurons of the above 4 groups ($n = 10$ neurons in each group). **D**, **E**, Cumulative frequency curves of interevent intervals (**D**) and means of mEPSC frequencies (**E**) in the above four groups. $n = 10$ neurons in each group. K–S test was used in **B** and **D**. ANOVA in **C** and **E**. $***, p < 0.001$; mean \pm standard error. The synaptic function is likely caused by the postsynaptic presence of tau due to the low transfection rate of the calcium phosphate precipitation method as presynaptic terminals are rarely transfected (see Materials and Methods and Teravskis et al., 2018, 2021 for previous characterizations).

amplitudes to the left (Fig. 4B; K–S test: $p < 0.001$ between wild-type 3R tau and G272V mutant 3R tau proteins). Consistent with results in Figure 4B, compared with wild-type 3R tau, the expression of G272V mutant 3R tau proteins significantly decreased the mEPSC amplitude from 19.1 to 12.8 pA (Fig. 4C; ANOVA, $F = 7.8$; Bonferroni's after test: $p < 0.001$). As a control, there is no significant difference between the mEPSC amplitudes of untransfected neurons and wild-type 3R tau-expressing neurons (Fig. 4C; ANOVA, $F = 7.8$; Bonferroni's after test: $p > 0.05$). In contrast, the expression of G272V mutant 4R tau proteins did not significantly shift the cumulative frequency curves of mEPSC amplitudes (Fig. 4B) and had no significant effects on the mean of mEPSC amplitudes (Fig. 4C; Bonferroni's after test: $p > 0.05$). These results indicate that the missorted G272V mutant 3R tau proteins induce loss of AMPARs in excitatory synapses, which is similar to a previously reported effect of P301L 4R tau (Hoover et al., 2010; Teravskis et al., 2021). However, it is unknown whether the missorted 3R and 4R tau proteins activate a common downstream pathway responsible for the weakening of excitatory synaptic responses.

In addition to changes in mEPSC amplitude, the expression of G272V mutant 3R tau proteins also alters mEPSC frequency. Compared with wild-type 3R tau, the expression of G272V mutant 3R tau proteins significantly shifted the cumulative frequency curve of interevent intervals to the right (Fig. 4D; K–S test: $p < 0.001$) and decreased the mEPSC frequency from 1.42 to 0.79 events/s (Fig. 4E; ANOVA, $F = 7.6$; Bonferroni's after test: $p < 0.001$ when compared with either untransfected or WT 3R tau controls). The changes in mEPSC frequency are consistent with a loss of dendritic spines as shown in Figure 3 (see Discussion). These results, together with results in Figure 3, demonstrate that the missorted G272V mutant 3R tau can impair both the structures and functions of dendritic spines, unraveling a new cellular mechanism underlying synaptic deficits in familial Pick's disease.

The G272V-induced 3R tau mislocalization depends upon tau phosphorylation

Previous studies have shown that the mislocalization of 4R tau to dendritic spines can be blocked by concurrent inhibition of two tau kinases, GSK3 β and CDK5 (Braun et al., 2020; Teravskis et al., 2021), which block phosphorylation of multiple serine/threonine sites of tau (Illenberger et al., 1998; Kimura et al., 2013, 2014). However, whether the mislocalization of 3R tau also depends upon the activation of similar kinases remains unknown. Therefore, we transfected neurons with plasmids encoding wild-type and G272V mutant 3R tau proteins (Fig. 5A). Next, 5-week-old neurons were incubated with both GSK3 β inhibitor, CHIR99021 (500 nM), and CDK5 inhibitor, Roscovitine (500 nM), for 24 h (Fig. 5A). As shown above, G272V mutant 3R proteins were mislocalized to dendritic spines and their expression decreased the density of these spines (Fig. 5A, second row). The concurrent treatment with CHIR99021 and CDK5 inhibitors blocks both cellular changes caused by the G272V mutation (Fig. 5A, third row). Compared with WT 3R tau, the expression of G272V mutant 3R tau proteins increased the proportion of dendritic spines that contained GFP-labeled tau versus the total number of spines labeled by DsRed from 18.9 to 83.7% (Fig. 5B, ANOVA, $F = 134.8$; Bonferroni's after test: $p < 0.001$) and concurrent treatment with both inhibitors blocked this change (Fig. 5B, from 83.7 to 19.0%; Bonferroni's after test: $p < 0.001$). This treatment also blocked the decrease in spine density caused by the G272V

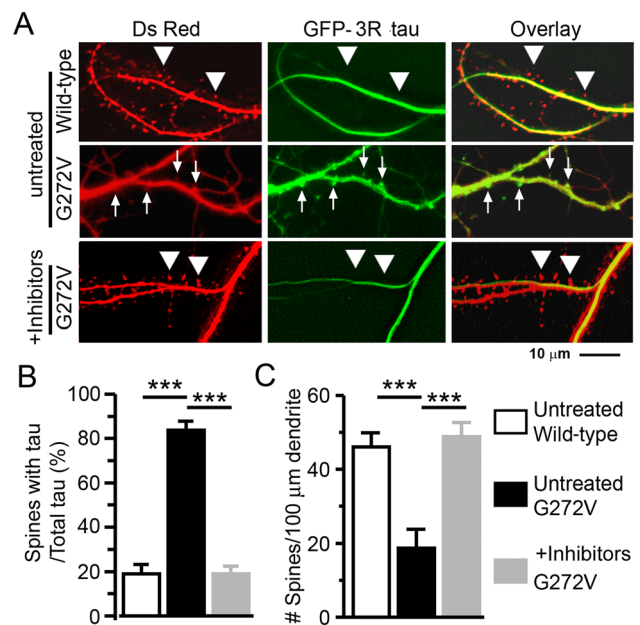


Figure 5. Pharmacological blockade of both GSK3 β and CDK5 tau kinases prevents mislocalization of G272V 3R tau proteins to dendritic spines and spine loss caused by this mutant protein. **A**, Five-week-old neurons that had been transfected with WT 3R tau with no drug treatment were used as the control (top row). Neurons coexpressing DsRed and GFP-tagged G272V 3R tau were untreated (middle row) or treated with a GSK3 β inhibitor, CHIR99021 (500 nM), and a CDK5 inhibitor, Roscovitine (500 nM) for 24 h (bottom row). **B**, Comparisons between the proportions of dendritic spines that contained tau versus the total number of DsRed-labeled spines in dendrites from the above groups. **C**, Comparisons between the densities of dendritic spines (number of spines per 100 μm length of dendrites) of the above groups. ANOVA, $n = 7$ neurons in each group, ***, $p < 0.001$; mean \pm standard error.

mutation (Fig. 5C, ANOVA, $F = 16.8$; from 17.8 in the untreated G272V group to 48.8 in the treated G272V group; Bonferroni's after test: $p < 0.001$). These results indicate that, like 4R tau, the mislocalization of G272V mutant 3R tau proteins to dendritic spines also depends upon the phosphorylation by GSK3 β and CDK5, suggesting shared upstream signaling steps before the mislocalization of both tau isoforms.

The electrophysiological deficits caused by G272V mutant 3R tau are dependent on tau phosphorylation

An additional functional study was performed in 5-week-old neurons expressing mutant G272V 3R tau to test whether functional deficits in dendritic spines are also dependent on tau phosphorylation. The neurons were incubated with and without both the GSK3 β inhibitor, CHIR99021 (500 nM), and the CDK5 inhibitor, Roscovitine (500 nM), for 1–3 d and subsequently patched to record mEPSCs (Fig. 6A, middle and bottom traces). Untransfected neurons with no treatment of the above inhibitors were included as a control (Fig. 6A, top trace). There were smaller and fewer mEPSC responses in neurons expressing G272V 3R proteins compared with the untransfected negative control as well as neurons that were concurrently treated with GSK3 β and CDK5 inhibitors (Fig. 6A). In contrast with the untransfected neurons, the expression of G272V mutant 3R tau shifted the cumulative curve of mEPSC amplitude to the left, and the pharmacological treatment inhibited this shifting (Fig. 6B; K–S test, $p < 0.001$ when compared with either the untransfected control or the treated 3R tau group). Consistent with the above curves, the expression of the mutant protein also significantly

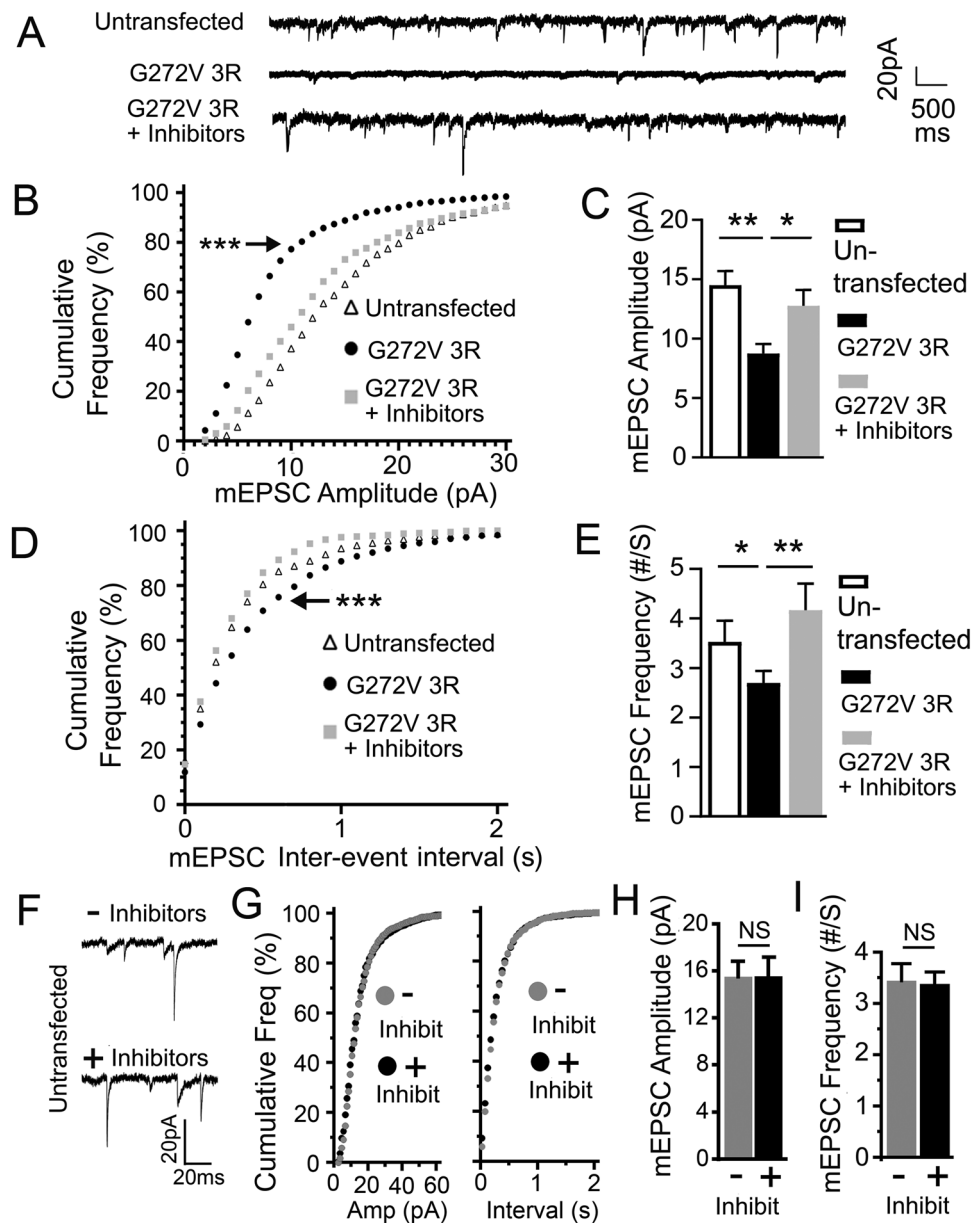


Figure 6. Pharmacological blockade of both GSK3 β and CDK5 tau kinases rescues synaptic dysfunction caused by G272V 3R tau. **A**, Representative traces from 5-week-old neurons that had been transfected with no plasmid (top) or G272V 3R tau (middle, no drug treatment; lower, treated with GSK3 β and CDK5 inhibitors). **B**, **C**, Cumulative curves and histograms of mEPSC amplitudes in three groups of neurons as described in **A**. In **B**, K–S tests were performed to compare neurons expressing G272V 3R tau with the untransfected control and the treated G272V 3R tau group. ***, $p < 0.001$ in both comparisons. In **C**, ANOVA analyses were performed to compare the means between the three groups ($n = 8–12$). *, $p < 0.05$; **, $p < 0.01$. **D**, **E**, Cumulative curves of interevent intervals and histograms of mEPSC frequencies in three groups of neurons as described in **A**. In **D**, K–S test; ***, $p < 0.001$ when the untreated G272V 3R was compared with the other two groups. In **E**, ANOVA test; *, $p < 0.05$; **, $p < 0.01$; mean \pm standard error. **F**, Representative traces of untransfected neurons without (top) or with (bottom) cotreatment with GSK3 β and CDK5 inhibitors. **G**, Cumulative frequency curves of the amplitudes (left) and interevent intervals (right) of mEPSCs from untreated and treated neurons (gray, no drug; black, with inhibitor treatment). **H**, **I**, Comparison of mEPSC amplitudes (**H**) and mEPSC frequency (**I**) between neurons without or with the treatment of inhibitors (gray and black, respectively). Two-group t test, $n = 14$ in each group, NS, not significant, $p > 0.05$; mean \pm standard error.

decreased the mean mEPSC amplitude (Fig. 6C; ANOVA test, $F = 10.9$, $p < 0.001$ overall; Bonferroni's after test: $p < 0.01$), and the pharmacological treatment inhibited this cellular change (Fig. 6C; Bonferroni's after test: $p < 0.05$). Similar changes also occurred in mEPSC frequency (Fig. 6D,E). In contrast with the untransfected neurons, the expression of G272V mutant 3R tau shifted the cumulative curve of interevent time interval to the right and the pharmacological treatment inhibited this shifting (Fig. 6D; K–S test, $p < 0.001$ when compared with either the untransfected control or the treated 3R tau group). Consistent

with the above curves, the expression of G272V 3R tau also significantly decreased the mean mEPSC frequency (Fig. 6E; ANOVA test, $F = 5.8$, $p < 0.001$ overall; Bonferroni's after test: $p < 0.05$), and the pharmacological treatment inhibited this cellular change (Fig. 6E; Bonferroni's after test: $p < 0.01$). In a negative control experiment (Fig. 6F–I), we found that cotreatment with GSK3 β and CDK5 inhibitors had no significant effects on either mEPSC amplitude or frequency. These data together demonstrate that the expression of mutant G272V 3R tau proteins decreased both the frequency and amplitude of mEPSCs whereas

the blockade of tau phosphorylation by the concurrent treatment with GSK3 β and CDK5 inhibitors reversed these synaptic dysfunctions. It indicates that 3R tau-mediated functional impairments of dendritic spines are also dependent upon tau phosphorylation by GSK3 β and CDK5.

The G272V mutation induces the formation of Pick body-like intracellular inclusions of 3R tau proteins in old cultured hippocampal neurons (5 weeks in vitro)

The extensive presence of Pick bodies is the pathological hallmark of both idiopathic and familial Pick's disease, and the definite diagnosis of this disease requires the detection of Pick bodies in the postmortem tissues (Kertesz et al., 2003; Cairns et al., 2007; Uchihara and Tsuchiya, 2008). In human tissues, Pick bodies are round or oval intracellular inclusions, consisting of aggregated 3R tau-containing network-like fibrils that are attached to the membrane surrounding the nucleus (Kovacs et al., 2013; Miki et al., 2014). To test whether the G272V mutation can induce accumulation of tau proteins next to the nucleus and the formation of the Pick body-like structures, we transfected neurons with plasmids encoding GFP-tagged wild-type, P301L and G272V 4R tau proteins (Fig. 7A), and GFP-tagged wild-type and G272V 3R tau (Fig. 7B). In our live imaging studies of dendrites (Figs. 1, 2), we had also looked at the somas for potential overt tau aggregations. We could not visually identify any overt Pick body-like structures in neurons at 3 weeks in vitro but started to see overt Pick body-like structures at 5 weeks in vitro. Accordingly, neurons at 5 weeks in vitro were fixed, permeabilized, and counterstained with DAPI to label the nuclei (see Materials and Methods). Among the transfections, only the expression of G272V mutant 3R tau proteins induced the formation of Pick body-like structures (Fig. 7B, bottom row). To test whether the G272V 3R tau caused asymmetrical aggregation of tau proteins, we visually identified the brightest side of the cytoplasm next to the nucleus and calculated its fluorescence intensity (F_1) and, at the same time, calculated the fluorescence intensity of the cytoplasm on the opposite side of the nucleus (F_2). We calculated the normalized difference between F_1 and F_2 as $(F_1 - F_2) / F_2$ for comparisons of the asymmetrical distribution of tau proteins between different transfections (Fig. 7C). We found that, compared with the wild-type 3R tau proteins, the expression of G272V mutant 3R tau significantly increased the accumulation of tau proteins on one side of the nucleus from 17.6 to 142.6%, causing the asymmetric distribution of tau proteins next to the nucleus (Fig. 7C, fifth column; ANOVA, $F = 11.0$; Bonferroni's after test: $p < 0.001$), which is consistent with the immunohistochemical results of a previously reported Pick's disease mouse model (Rockenstein et al., 2015). Moreover, cotreatment with GSK3 β and CDK5 inhibitors, CHIR99021 (500 nM) and Roscovitine (500 nM), for 2 weeks (applied at 3 weeks in vitro; fixed at 5 weeks in vitro) mostly blocked the asymmetric accumulation of 3R G272V tau proteins around the nucleus (Fig. 7B, bottom row; Fig. 7C, sixth column). Our results demonstrate a temporal association between the formation of Pick body-like asymmetrical aggregation of 3R tau proteins and deficits in synaptic structures and functions, supporting the disease relevance of our cellular studies here. Our pharmacological studies also support the role of tau phosphorylation in the formation of Pick bodies, which is consistent with human pathologies, showing that tau proteins in Pick bodies are highly phosphorylated (Kovacs et al., 2013; Miki et al., 2014). The pharmacological results further support the disease relevance of our mechanistic studies here.

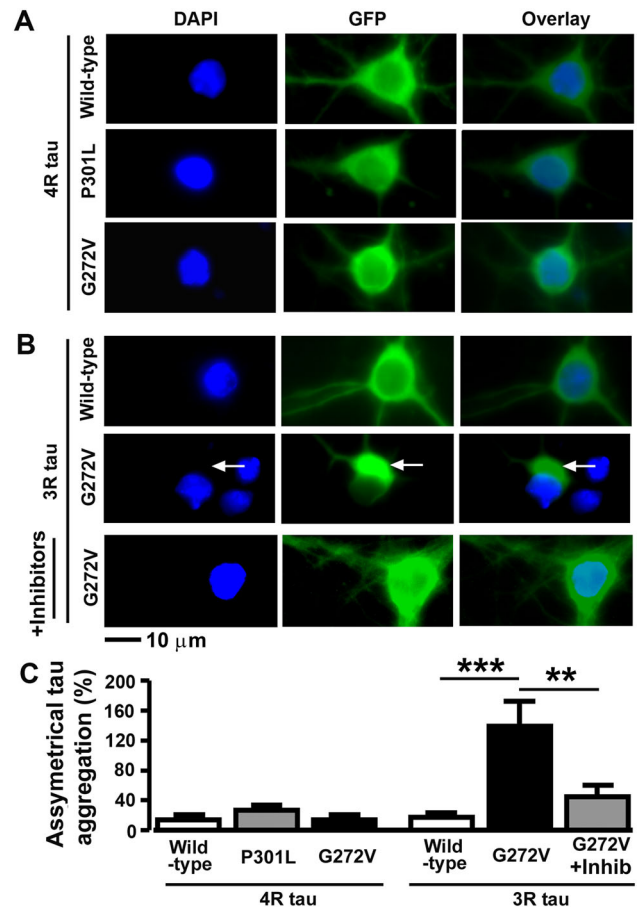


Figure 7. The G272V mutation induces the phosphorylation-dependent formation of Pick body-like structures by causing asymmetric accumulation of 3R tau proteins next to the nucleus. **A**, **B**, Representative images of 5-week-old cultured neurons expressing various GFP-tagged 4 R (**A**) and 3 R (**B**) tau proteins, which had been fixed and stained with DAPI to label the nucleus (see Materials and Methods). The bottom row of **B** shows a neuron expressing 3R G272V tau that had been treated with CDK5 and GSK3 β inhibitors. The arrows denote a Pick body-like structure on one side of the nucleus. **C**, The quantification of the asymmetrical distributions of tau in neurons expressing various types of tau proteins without or with inhibitor treatment (see main text). ANOVA, $n = 7$ neurons in each group, **, $p < 0.01$; ***, $p < 0.001$; mean \pm standard error.

The phosphorylation of 3R tau caused by the G272V mutation has a slower temporal dynamic than that of 4R tau caused by the P301L mutation

Unlike P301L, the G272V mutation induced tau mislocalization to dendritic spines as early as 3 weeks in vitro but had a delayed effect on synaptic functions of neurons in 5 weeks in vitro (Figs. 1–4). In our previous study, we found that 4R tau-mediated synaptic dysfunction by two stepwise cellular changes: tau mislocalization to dendritic spines and subsequent loss of synaptic AMPARs (Teravskis et al., 2021). While tau mislocalization depends on the phosphorylation of the C-domain (Ser396/Ser404), loss of functional AMPARs instead depends upon the phosphorylation of the B-domain (i.e., Ser202, Thr205, Thr212, Thr217, and Thr231; Teravskis et al., 2021). Therefore, we hypothesized that the delayed functional deficits caused by 3R G272V tau result from a delayed phosphorylation of the B-domain. To test the hypothesis, we utilized the AT8 anti-tau antibody to detect the phosphorylation of the Ser202/Thr205 in tau and a polyclonal anti-GFP antibody to detect the amount of expressed GFP-tagged human tau levels in neurons at ages of 3 and 5 weeks in vitro, respectively (Fig. 8A,B; see

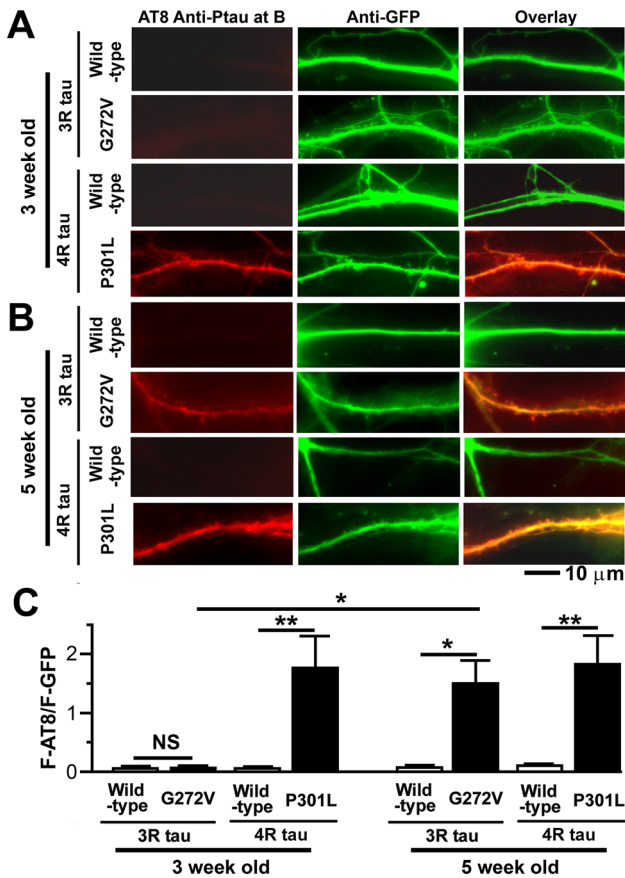


Figure 8. The phosphorylation of the B-domain in 3R tau caused by the G272V mutation is slower than that in 4R tau caused by the P301L mutation. **A**, Representative images of 3-week-old cultured neurons expressing various GFP-tagged 3R (top 2 rows) and 4R (bottom 2 rows) tau proteins. The neurons were costained with the mouse AT8 antibody to detect the phosphorylation of Ser202/Ser205 in tau (part of the B-domain as described in Teravskis et al., 2021) and a rabbit polyclonal anti-GFP antibody to detect total tau, respectively. **B**, Images that are similar to those in **A** but at an older age of 5 weeks in vitro. **C**, Comparison of AT8 staining (normalized by GFP staining) between eight groups of neurons as described in **A** and **B** (see Materials and Methods for quantification equations). Two-way ANOVA, $n = 8$ neurons in each group; Factor 1 = 2 ages; Factor 2 = 4 tau variants. Overall results, Overall model, $F = 8.5$, $p < 0.001$; means in Factor 2, $p < 0.001$; interaction between two factors, $p < 0.05$. Individual group comparison in **C**, NS, not significant, $p > 0.05$; *, $p < 0.05$; **, $p < 0.01$; mean \pm standard error.

Materials and Methods). In each fluorescence channel, the normalized intensity of dendritic fluorescence $F = (F_{\text{neuron}} - F_{\text{background}}) / F_{\text{background}}$ (see Materials and Methods). Thereafter, we further calculated the ratio of normalized fluorescence intensity of AT8 staining (F-AT8) over the normalized GFP fluorescence (F-GFP; Fig. 8C). In order to determine the effects of both neuronal age and tau variants, we used the two-way ANOVA to compare the means of the above ratio between 8 groups of neurons (Factor 1 = 2 ages; Factor 2 = 4 tau variants; $2 \times 4 = 8$; Fig. 8C). We found that the two factors together significantly altered the ratio among groups (sample size, $n = 8$ neurons in each group; overall model, $F = 8.5$, $p < 0.001$). The means between the four levels of Factor 2 ($2 \times 2 = 4$; two isoforms and two mutations) are significantly different ($p < 0.001$), indicating that the G272V and/or P301L mutations can indeed alter the phosphorylation of tau in the B-domain. The interaction between the two factors is also significant ($p < 0.05$), indicating that the age of neurons can modulate the effects of the two mutations on the phosphorylation of the B-domain in tau. In the

comparison between individual groups, the G272V mutation significantly increases the AT8 staining of 3R tau in the older cultures (5 weeks old; Fig. 8C, fifth and sixth bars) but not in the younger cultures (3 weeks old; Fig. 8C, first and second bars). In contrast, the P301L mutation significantly increases the AT8 staining of 4R tau in neurons at both ages (the third, fourth, seventh, and eighth bars). These results indicate that the phosphorylation of the B-domain caused by the G272V mutation is slower than that by the P301L mutation, supporting the hypothesis that the delayed synaptic dysfunction caused by the G272V mutation is likely due to a delayed phosphorylation of the B-domain.

The expression of G272V 3R tau and P301L 4R tau proteins induces deficits in AMPAR-mediated synaptic responses through dynamin-dependent and dynamin-independent mechanisms, respectively

Previous publications have extensively reported that excitatory postsynaptic responses can be weakened by dynamin-dependent clathrin-mediated endocytosis of synaptic AMPARs (Carroll et al., 1999; Lüscher et al., 1999; Man et al., 2000; Anggono and Huganir, 2012). To test the role of the above pathway in 3R and 4R tau pathophysiology, we first transfected 1-week-old neurons with either G272V 3R tau or P301L 4R tau, allowing the neurons to age. Thereafter, we treated the 4–5-week-old neurons with dynasore (15 μM ; see Materials and Methods), which is an inhibitor of both dynamin 1 and dynamin 2, for 1–2 d for electrophysiological studies (Macia et al., 2006; Fig. 9A, six groups of experiments).

Consistent with our prior results, the expression of G272V 3R tau proteins significantly shifted the cumulative frequency curve of mEPSC amplitudes to the left (Fig. 9B; K-S test: $p < 0.001$ between G272V 3R tau proteins and the untransfected control with no drug treatment). Consistent with results in Figure 9B, compared with untransfected control with no drug treatment, the expression of G272V 3R tau proteins significantly decreased the mEPSC amplitude from 18.5 to 12.6 pA (Fig. 9D, left four bars; $n = 12$ –14 neurons; ANOVA, $F = 7.9$; Bonferroni's after test: $p < 0.001$). The dynasore treatment blocked the shifting of the G272V 3R tau cumulative curve in Figure 9B and the decrease in mEPSC amplitude caused by this mutant in Figure 9D. The results in Figure 9, B and D, collectively indicate that the G272V 3R tau proteins induce loss of AMPARs in excitatory synapses, and this impairment is dynamin-dependent.

In addition to changes in mEPSC amplitude, the expression of G272V 3R tau proteins also shifted the cumulative curve of mEPSC inter-event interval to the right (Fig. 9B; K-S test: $p < 0.001$) and decreased the mean of mEPSC frequency from 2.07 to 0.93 events/s (Fig. 9E, left four bars; ANOVA, $F = 17.2$; Bonferroni's after test: $p < 0.001$ when compared with the untransfected control with no drug treatment). The changes in mEPSC frequency are consistent with a loss of dendritic spines as shown in Figure 3 (see Discussion). Importantly, this decrease in mEPSC frequency was not blocked by dynasore (Fig. 9B,E), suggesting that dynamin likely plays little role in 3R tau-mediated spine loss.

The expression of P301L 4R tau proteins significantly shifted the cumulative frequency curve of mEPSC amplitudes to the left (Fig. 9C; K-S test: $p < 0.001$ between the mutant 4R tau and the untransfected control with no drug treatment). Consistent with results in Figure 9C, compared with the untransfected control with no drug treatment, the expression of P301L 4R tau proteins significantly decreased the mean of mEPSC amplitude from 18.5 to 11.2 pA (Fig. 9D, right four bars; $n = 12$ –14 neurons; ANOVA,

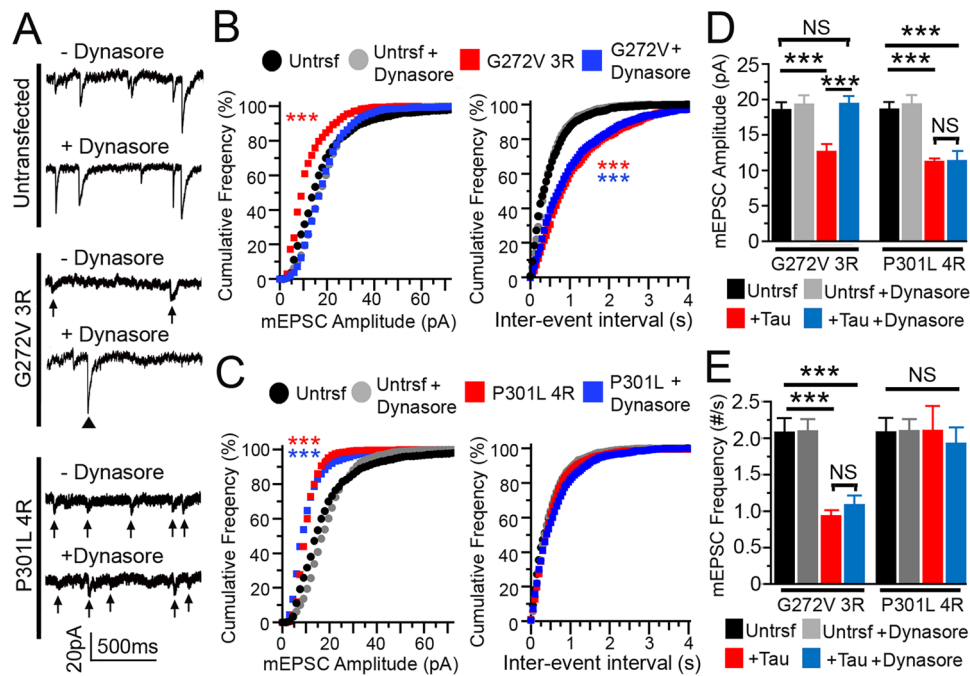


Figure 9. G272V 3R tau and P301L 4R tau impair AMPAR-mediated synaptic responses through dynamin-dependent and dynamin-independent mechanisms, respectively. **A**, Representative traces from 4 to 5-week-old neurons that had been transfected with no plasmid (top), G272V 3R tau (middle), or P301L 4R tau (bottom) with (+) or without (–) dynasore treatment (15 μ M; see Materials and Methods, Pharmacology). The arrows denote suppressed synaptic responses, and the triangle denotes a rescuing effect of dynasore. **B**, Cumulative curves of mEPSC amplitudes (left) and interevent time interval (right) from four groups of neurons (untransfected with or without dynasore; transfected with G272V 3R tau with or without dynasore; labeled with 4 colored symbols on the top). **C**, Similar cumulative curves as in **B** from four different groups of neurons (untransfected with or without dynasore; transfected with P301L 4R tau with or without dynasore). **D**, Comparison of mEPSC amplitudes between four groups of neurons in two sets of experiments [left four bars, untransfected (black), untransfected + dynasore treatment (gray), G272V 3R (red), and G272V 3R + dynasore treatment (blue); right four bars, untransfected (black), untransfected + dynasore treatment (gray), P301L 4R tau (red), and P301L 4R tau + dynasore treatment (blue)]. **E**, Comparison of mEPSC frequencies between 4 groups of neurons in two same sets of experiments as in **D**. In **B** and **C**, K–S tests were performed to compare the cumulative curves with the control curves (no transfection, no drug treatment). In **D** and **E**, one-way ANOVA tests were performed to compare the means of four groups in each set of experiments. ***, $p < 0.001$; NS, not significant, $p > 0.05$.

$F = 17.1$; Bonferroni’s after test: $p < 0.001$). However, unlike G272V 3R tau, the expression of P301L 4R tau did not significantly decrease the mEPSC frequency (Fig. 9C and Fig. 9E, right four bars; $p > 0.05$ across all groups in ANOVA). In our pharmacological studies, the dynasore treatment at a concentration of 15 mM did not block the P301L 4R tau-induced decrease in mEPSC amplitude (Fig. 9D, right four bars). Therefore, the above pharmacological studies of both G272V 3R tau– and P301L 4R tau–expressing neurons together indicate that 3R and 4R tau proteins likely mediate functional deficits of dendritic spines through distinct dynamin-dependent and dynamin-independent mechanisms, respectively.

Discussion

Here, we demonstrate that either 3R tau or 4R tau proteins can be mislocalized to dendritic spines but by different pathogenic variants (Figs. 1, 3). Dendritic spines are postsynaptic structures of glutamatergic synapses (Harris and Kater, 1994; Kennedy, 2000), and the plasticity of these synapses is the most studied cellular model of learning and memory (Malenka, 1994; Martin et al., 2000). Deficits in dendritic spines have been widely proposed to account for cognitive deficits in AD and other tauopathies (Hoover et al., 2010; Ittner et al., 2010; Müller et al., 2014; Teravskis et al., 2018; Braun et al., 2020). We performed a systemic comparison between the roles of 3R and 4R tau in modulating the structures and functions of dendritic spines. Our results provide direct evidence showing that tau mislocalization

to dendritic spines is a common cellular change in models of 3R and 4R tau FTD.

However, after being mislocalized to dendritic spines, 3R and 4R tau proteins are likely to impair the functions and structures of these spines through different downstream pathways. The G272V mutant 3R tau decreased both the amplitude and frequency of mEPSCs (Fig. 4), which are consistent with the loss of AMPARs and the loss of dendritic spines, respectively. In the classical mathematical model (Del Castillo and Katz, 1954), a decrease in mEPSC amplitude reflects the loss of postsynaptic receptors whereas a decrease in mEPSC frequency reflects a decrease in releasing probability or loss of releasing sites (secondary to loss of attached presynaptic terminals caused by spine loss). The G272V-induced tau mislocalization to dendritic spines and associated functional deficits are 3R tau specific as G272V 4R tau caused no functional deficits (Figs. 1–4). Unlike the P301L 4R tau, the expression of G272V 3R tau also caused additional spine loss (Fig. 3). We also found that only the G272V mutation but not the P301L mutation induced the formation of Pick body–like structures next to the nucleus (Fig. 7). Finally, we found that the decrease in mEPSC amplitude caused by G272V 3R tau is dynamin-dependent but that by P301L 4R tau is not, supporting distinct cellular mechanisms (Fig. 9). These results together suggest that although some steps in the upstream of tau mislocalization may be the same, the downstream signaling steps are likely to be different.

The above difference is supported by human studies, showing that the P301L tau mutation is associated with neurofibrillary

tangles of hyperphosphorylated 4R tau whereas the G272V mutation is associated with 3R tau-containing Pick bodies (Bronner et al., 2005; Ghetti et al., 2015). The Pick bodies are round or oval intracellular inclusions of aggregated 3R tau network-like fibrils attached to the nuclear membrane (Kovacs et al., 2013; Miki et al., 2014). As shown in Figure 7, the G272V mutation increased the asymmetric accumulation of 3R tau proteins next to the nucleus to form Pick body-like structures, recapitulating the pathological hallmarks of human Pick's disease and supporting the disease relevance of this study.

The pathological progression speed from the transfection of G272V 3R tau to observed functional deficits is also different from that of P301L 4R tau (Figs. 2, 4). In our previous study, after transfection at 1 week in vitro, the expression of P301L 4R tau induced deficits in synaptic responses in electrophysiology and loss of AMPARs in immunocytochemistry in 3-week-old cultured hippocampal neurons (Hoover et al., 2010). Here, the expression of G272V 3R tau instead caused no overt synaptic impairment in 3-week-old cultured neurons but profoundly impaired the structures and functions of dendritic spines in older cultures (5 weeks in vitro), showing that functional changes caused by 3R tau are slower than those of 4R tau. Our cellular study is consistent with a previous clinical comparative study that showed a relatively slower disease progression of 3R tauopathies than 4R tauopathies (Hu et al., 2007).

The precise molecular structural basis for why G272V mutation causes isoform-specific tau mislocalization to dendritic spines remains to be clarified. The G272V and P301L mutations affect the same PGGG motif in a similar position within the first and second microtubule-binding domains, respectively, altering this motif to PGVG or LGGG (Yamaoka et al., 1996; Hutton et al., 1998). Here, the whole second microtubule-binding domain is artificially truncated by PCR mutagenesis in the 3R tau proteins (Fig. 1A). Moving the mutant PGVG motif closer to the S396/S404 sites, which are essential for tau mislocalization (Teravskis et al., 2021), by the above truncation may facilitate the phosphorylation of these sites in G272V 3R tau, leading to the observed tau mislocalization.

Our pharmacological results (Figs. 5, 6) indicate that the immediate upstream signaling molecules that mediate 3R tau hyperphosphorylation are likely GSK3 β and CDK5, which are two of the best-known tau kinases that play important roles in AD and other neurodegenerative diseases (Ishiguro et al., 1993; Patrick et al., 1999; Hernandez et al., 2013). G272V-induced 3R tau mislocalization to dendritic spines and associated synaptic deficits were blocked by concurrent incubation with inhibitors of these two kinases (Figs. 5, 6). Our previous cellular study demonstrates that the mislocalization of 4R tau caused by P301L mutation requires the phosphorylation of S396/S404 residues in the C-terminus of the 4R tau (Teravskis et al., 2021). Therefore, the mislocalization of 3R tau is likely to be mediated through a shared phosphorylation-dependent cellular mechanism as S396/S404 are major tau substrates of GSK3 β and CDK5 (Illenberger et al., 1998; Kimura et al., 2013, 2014), which can be activated by endoplasmic reticulum stress (Lai et al., 2007; Liu et al., 2016; Su et al., 2016; Kim et al., 2017). The GSK3 β and CDK5-mediated mislocalization of 3R tau may also play a role in AD and CTE because both diseases exhibit mixed 3R and 4R tau pathologies (Hasegawa et al., 2014; Arena et al., 2020) whereas the phosphorylation of S396/S404 is among the earliest and most robust changes in AD (Mondragón-Rodríguez et al., 2014; Wesseling et al., 2020).

The signaling cascade downstream from mislocalization of 3R or 4R tau is largely unknown. One consistent scientific observation from multiple groups is that tau mislocalization to dendritic spines is associated with concurrent targeting to and clustering of the Fyn kinases in these spines (Ittner et al., 2010; Xia et al., 2015; Padmanabhan et al., 2019). The tyrosine phosphorylation of NR2B by Fyn increases the synaptic retention of NR2B (Prybylowski et al., 2005), and Fyn is believed to be an important mediator/modulator of long-term potentiation (Grant et al., 1992; Lu et al., 1999). The accumulation of Fyn in dendritic spines in an AD model is associated with loss of dendritic spines and cognitive deficits (Um et al., 2012). However, how Fyn leads to impairments of dendritic spines in neurodegenerative diseases remains unknown. The nano-clustered Fyn may cause loss of functional AMPARs by inhibiting AMPAR trafficking to postsynaptic membranes during LTP, enhancing AMPAR internalization via calcineurin, or other mechanisms (illustrated in Fig. 10). In addition, 3R tau and/or Fyn may cause collapse of dendritic spines by modulating the activities of small GTPases, which are major players in spine morphogenesis (Luo et al., 1996; Nakayama et al., 2000; Wiens et al., 2005).

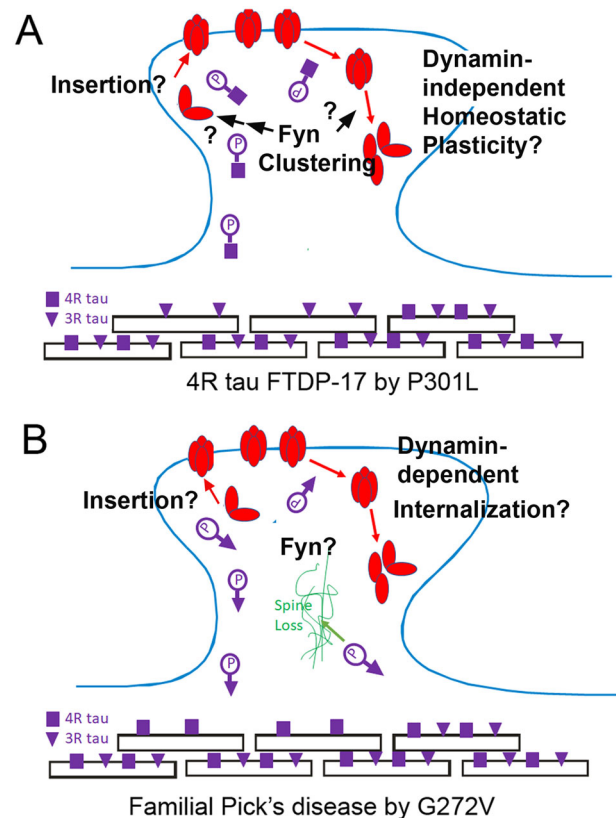


Figure 10. Hypothetical models for the roles of tau mislocalization in 4R tau FTD and 3R tau FTD (Pick's disease). **A**, In 4R tau FTDP-17 caused by P301L mutation, 4R tau proteins were phosphorylated and mislocalized to dendritic spines, which brings Fyn proteins to dendritic spines (Ittner et al., 2010; Xia et al., 2015; Padmanabhan et al., 2019). The postsynaptic nano-clustering of Fyn may lead to the loss of AMPARs via an unknown dynamin-independent mechanism. **B**, In familial Pick's disease (also called 3R tau FTDP-17), the phosphorylation of 3R tau leads to tau mislocalization to dendritic spines and subsequent loss of functional AMPARs in postsynaptic membranes via dynamin-dependent clathrin-mediated AMPAR endocytosis. The mislocalized 3R tau proteins may also directly or indirectly interact with actin, leading to the loss of dendritic spines. However, it remains to be determined whether 3R tau mislocalization is also associated with the postsynaptic nano-clustering of Fyn.

In studies of the downstream pathway here (Fig. 9), we found that deficits in AMPAR-mediated synaptic responses caused by 3R and 4R tau are dynamin-dependent and dynamin-independent, respectively. Dynamin plays an essential role in clathrin-mediated endocytosis, which is an intracellular signal machinery highly conserved across species and cell types (Mousavi et al., 2004; Doherty and McMahon, 2009). Much is known about the role of the rapid dynamin-dependent clathrin-mediated internalization of AMPARs during long-term depression, a form of Hebbian synaptic plasticity (Carroll et al., 1999; Lüscher et al., 1999; Man et al., 2000; Anggono and Huganir, 2012). However, increasing evidence in recent years demonstrates that constitutive AMPAR internalization and homeostatic AMPAR downscaling do not require the function of dynamin and clathrin (Glebov et al., 2015; Zheng et al., 2015). In Figure 9, the contrasting effects of dynasore, a dynamin inhibitor, on mEPSC amplitudes of neurons that expressed G272V 3R tau and P301L 4R tau proteins suggest that 3R and 4R tau isoforms interfere with different recycling pathways of AMPARs, affecting Hebbian and homeostatic synaptic plasticity, respectively (illustrated in Fig. 10).

In conclusion, our findings elucidate that tau mislocalization to dendritic spines is a common pathway for both 3R and 4R tau proteins to impair postsynaptic structures and functions but through different downstream mechanisms (illustrated in Fig. 10). The shared upstream steps that lead to mislocalization of 3R and 4R tau provide a common cellular mechanism underlying frequent overlaps of clinical presentations in diverse forms of FTD. On the other hand, the uncovered dynamin-dependent and dynamin-independent downstream mechanisms activated by 3R and 4R tau, respectively, provide an unreported molecular and cellular framework for the pathophysiological heterogeneity of FTD. Broadly, the comparative mechanistic studies of diverse tau isoforms here will help us better understand the complexity of cellular mechanisms underlying diverse neurodegenerative diseases, which may exhibit 3R, 4R, or both tau pathologies.

Data availability. Data in support of the findings here are available from the corresponding author with reasonable request.

References

- Andreadis A (2005) Tau gene alternative splicing: expression patterns, regulation and modulation of function in normal brain and neurodegenerative diseases. *Biochim Biophys Acta* 1739:91–103.
- Andreadis A, Brown WM, Kosik KS (1992) Structure and novel exons of the human tau gene. *Biochemistry* 31:10626–10633.
- Anggono V, Huganir RL (2012) Regulation of AMPA receptor trafficking and synaptic plasticity. *Curr Opin Neurobiol* 22:461–469.
- Arena JD, Smith DH, Lee EB, Gibbons GS, Irwin DJ, Robinson JL, Lee VM, Trojanowski JQ, Stewart W, Johnson VE (2020) Tau immunophenotypes in chronic traumatic encephalopathy recapitulate those of ageing and Alzheimer's disease. *Brain* 143:1572–1587.
- Bang J, Spina S, Miller BL (2015) Frontotemporal dementia. *Lancet* 386:1672–1682.
- Braun NJ, Yao KR, Alford PW, Liao D (2020) Mechanical injuries of neurons induce tau mislocalization to dendritic spines and tau-dependent synaptic dysfunction. *Proc Natl Acad Sci U S A* 117:29069–29079.
- Bronner IF, ter Meulen BC, Azmani A, Severijnen LA, Willemsen R, Kamphorst W, Ravid R, Heutink P, van Swieten JC (2005) Hereditary Pick's disease with the G272V tau mutation shows predominant three-repeat tau pathology. *Brain* 128:2645–2653.
- Butner K, Kirschner M (1991) Tau protein binds to microtubules through a flexible array of distributed weak sites. *J Cell Biol* 115:717–730.
- Cairns NJ, et al. (2007) Neuropathologic diagnostic and nosologic criteria for frontotemporal lobar degeneration: consensus of the consortium for frontotemporal lobar degeneration. *Acta Neuropathol* 114:5–22.
- Carroll RC, Beattie EC, Xia H, Lüscher C, Altschuler Y, Nicoll RA, Malenka RC, von Zastrow M (1999) Dynamin-dependent endocytosis of ionotropic glutamate receptors. *Proc Natl Acad Sci U S A* 96:14112–14117.
- Del Castillo J, Katz B (1954) Quantal components of the end-plate potential. *J Physiol* 124:560–573.
- Dickson DW, Kouri N, Murray ME, Josephs KA (2011) Neuropathology of frontotemporal lobar degeneration-tau (FTLD-tau). *J Mol Neurosci* 45:384–389.
- Doherty GJ, McMahon HT (2009) Mechanisms of endocytosis. *Annu Rev Biochem* 78:857–902.
- Dregni AJ, Duan P, Xu H, Changolkar L, El Mammeri N, Lee VM, Hong M (2022) Fluent molecular mixing of tau isoforms in Alzheimer's disease neurofibrillary tangles. *Nat Commun* 13:2967.
- Ghetti B, Oblak AL, Boeve BF, Johnson KA, Dickerson BC, Goedert M (2015) Invited review: frontotemporal dementia caused by microtubule-associated protein tau gene (MAPT) mutations: a chameleon for neuropathology and neuroimaging. *Neuropathol Appl Neurobiol* 41:24–46.
- Glebov OO, Tigaret CM, Mellor JR, Henley JM (2015) Clathrin-independent trafficking of AMPA receptors. *J Neurosci* 35:4830–4836.
- Goedert M, Jakes R, Vanmechelen E (1995) Monoclonal antibody AT8 recognizes tau protein phosphorylated at both serine 202 and threonine 205. *Neurosci Lett* 189:167–169.
- Goode B, Denis P, Panda D, Radeke M, Miller H, Wilson L, Feinstein S (1997) Functional interactions between the proline-rich and repeat regions of tau enhance microtubule binding and assembly. *Mol Biol Cell* 8:353–365.
- Grant SG, O'Dell TJ, Karl KA, Stein PL, Soriano P, Kandel ER (1992) Impaired long-term potentiation, spatial learning, and hippocampal development in *fyn* mutant mice. *Science* 258:1903–1910.
- Hamos JE, DeGennaro LJ, Drachman DA (1989) Synaptic loss in Alzheimer's disease and other dementias. *Neurology* 39:355–361.
- Harris KM, Kater SB (1994) Dendritic spines: cellular specializations imparting both stability and flexibility to synaptic function. *Annu Rev Neurosci* 17:341–371.
- Hasegawa M, Watanabe S, Kondo H, Akiyama H, Mann DM, Saito Y, Murayama S (2014) 3R and 4R tau isoforms in paired helical filaments in Alzheimer's disease. *Acta Neuropathol* 127:303–305.
- Hernandez F, Lucas JJ, Avila J (2013) GSK3 and tau: two convergence points in Alzheimer's disease. *J Alzheimers Dis* 33:S141–S144.
- Heutink P, Stevens M, Rizzu P, Bakker E, Kros JM, Tibben A, Niermeijer MF, Van Duijn CM, Oostra BA, Van Swieten JC (1997) Hereditary frontotemporal dementia is linked to chromosome 17q21-22. A genetic and clinico-pathological study of three Dutch families. *Annu Neurol* 41:150–159.
- Hoover BR, et al. (2010) Tau mislocalization to dendritic spines mediates synaptic dysfunction independently of neurodegeneration. *Neuron* 68:1067–1081.
- Hu WT, Parisi JE, Knopman DS, Boeve BF, Dickson DW, Ahlskog JE, Petersen RC, Josephs KA (2007) Clinical features and survival of 3R and 4R tauopathies presenting as behavioral variant frontotemporal dementia. *Alzheimer Dis Assoc Disord* 21:S39–S43.
- Hutton M, et al. (1998) Association of missense and 5'-splice-site mutations in tau with the inherited dementia FTDP-17. *Nature* 393:702–705.
- Illenberger S, Zheng-Fischhöfer Q, Preuss U, Stamer K, Baumann K, Trinczek B, Biernat J, Godemann R, Mandelkow EM, Mandelkow E (1998) The endogenous and cell cycle-dependent phosphorylation of tau protein in living cells: implications for Alzheimer's disease. *Mol Biol Cell* 9:1495–1512.
- Iseki E, Togo T, Suzuki K, Katsuse O, Marui W, de Silva R, Lees A, Yamamoto T, Kosaka K (2003) Dementia with Lewy bodies from the perspective of tauopathy. *Acta Neuropathol* 105:265–270.
- Ishiguro K, Shiratsuchi A, Sato S, Omori A, Arioka M, Kobayashi S, Uchida T, Imahori K (1993) Glycogen synthase kinase 3 beta is identical to tau protein kinase I generating several epitopes of paired helical filaments. *FEBS Lett* 325:167–172.
- Ittner LM, et al. (2010) Dendritic function of tau mediates amyloid- β toxicity in Alzheimer's disease mouse models. *Cell* 142:387–397.
- Kennedy MB (2000) Signal-processing machines at the postsynaptic density. *Science* 290:750–754.
- Kertesz A, Hillis A, Munoz DG (2003) Frontotemporal degeneration, Pick's disease, Pick complex, and Ravel. *Ann Neurol* 54:S1–S2.
- Kim E, Sakata K, Liao FF (2017) Bidirectional interplay of HSF1 degradation and UPR activation promotes tau hyperphosphorylation. *PLoS Genet* 13:e1006849.

- Kimura T, et al. (2013) Isomerase Pin1 stimulates dephosphorylation of tau protein at cyclin-dependent kinase (Cdk5)-dependent Alzheimer phosphorylation sites. *J Biol Chem* 288:7968–7977.
- Kimura T, Ishiguro K, Hisanaga S (2014) Physiological and pathological phosphorylation of tau by Cdk5. *Front Mol Neurosci* 7:65.
- Kolarova M, García-Sierra F, Bartos A, Ricny J, Ripova D (2012) Structure and pathology of tau protein in Alzheimer disease. *Int J Alzheimers Dis* 2012:731526.
- Kosik KS, Orecchio LD, Bakalis S, Neve RL (1989) Developmentally regulated expression of specific tau sequences. *Neuron* 2:1389–1397.
- Kovacs GG, et al. (2013) Neuropathology of the hippocampus in FTLT-D-Tau with Pick bodies: a study of the BrainNet Europe consortium. *Neuropathol Appl Neurobiol* 39:166–178.
- Lai E, Teodoro T, Volchuk A (2007) Endoplasmic reticulum stress: signaling the unfolded protein response. *Physiology* 22:193–201.
- Lin H, Higgins P, Loh HH, Law PY, Liao D (2009) Bidirectional effects of fentanyl on dendritic spines and AMPA receptors depend upon the internalization of mu opioid receptors. *Neuropsychopharmacology* 34:2097–2111.
- Lin H, Haganir R, Liao D (2004) Temporal dynamics of NMDA receptor-induced changes in spine morphology and AMPA receptor recruitment to spines. *Biochem Biophys Res Commun* 316:501–511.
- Ling SC, Polymenidou M, Cleveland DW (2013) Converging mechanisms in ALS and FTD: disrupted RNA and protein homeostasis. *Neuron* 79:416–438.
- Lippa CF (2004) Synaptophysin immunoreactivity in Pick's disease: comparison with Alzheimer's disease and dementia with Lewy bodies. *Am J Alzheimers Dis Other Dement* 19:341–344.
- Lippa CF, Hamos JE, Pulaski-Salo D, DeGennaro LJ, Drachman DA (1992) Alzheimer's disease and aging: effects on perforant pathway perikarya and synapses. *Neurobiol Aging* 13:405–411.
- Liu ZC, et al. (2016) SIL1 rescued Bip elevation-related tau hyperphosphorylation in ER stress. *Mol Neurobiol* 35:983–994.
- Lu YF, Kojima N, Tomizawa K, Moriwaki A, Matsushita M, Obata K, Matsui H (1999) Enhanced synaptic transmission and reduced threshold for LTP induction in *fyn*-transgenic mice. *Eur J Neurosci* 11:75–82.
- Luo L, Hensch T, Ackerman L, Barbel S, Jan L, Jan Y (1996) Differential effects of the Rac GTPase on Purkinje cell axons and dendritic trunks and spines. *Nature* 379:837–840.
- Lüscher C, Xia H, Beattie EC, Carroll RC, von Zastrow M, Malenka RC, Nicoll RA (1999) Role of AMPA receptor cycling in synaptic transmission and plasticity. *Neuron* 24:649–658.
- Macia E, Ehrlich M, Massol R, Boucrot E, Brunner C, Kirchhausen T (2006) Dynasore, a cell-permeable inhibitor of dynamin. *Dev Cell* 10:839–850.
- Malenka RC (1994) Synaptic plasticity in the hippocampus: LTP and LTD. *Cell* 78:535–538.
- Man HY, Lin JW, Ju WH, Ahmadian G, Liu L, Becker LE, Sheng M, Wang YT (2000) Regulation of AMPA receptor-mediated synaptic transmission by clathrin-dependent receptor internalization. *Neuron* 25:649–662.
- Martin SJ, Grimwood PD, Morris RGM (2000) Synaptic plasticity and memory: an evaluation of the hypothesis. *Annu Rev Neurosci* 23:649–711.
- Miki Y, Mori F, Tanji K, Kurotaki H, Kakita A, Takahashi H, Wakabayashi K (2014) An autopsy case of incipient Pick's disease: immunohistochemical profile of early-stage Pick body formation. *Neuropathology* 34:386–391.
- Miller EC, Teravskis PJ, Dummer BW, Zhao X, Haganir RL, Liao D (2014) Tau phosphorylation and tau mislocalization mediate soluble A β oligomer-induced AMPA glutamate receptor signaling deficits. *Eur J Neurosci* 39:1214–1224.
- Mondragón-Rodríguez S, Perry G, Luna-Muñoz J, Acevedo-Aquino MC, Williams S (2014) Phosphorylation of tau protein at sites Ser(396-404) is one of the earliest events in Alzheimer's disease and Down syndrome. *Neuropathol Appl Neurobiol* 40:121–135.
- Mousavi SA, Malerod L, Berg T, Kjekens R (2004) Clathrin-dependent endocytosis. *Biochem J* 377:1–16.
- Nakayama A, Harms M, Luo L (2000) Small GTPases Rac and Rho in the maintenance of dendritic spines and branches in hippocampal pyramidal neurons. *J Neurosci* 20:5329–5338.
- Padmanabhan P, Martínez-Mármol R, Xia D, Götz J, Meunier FA (2019) Frontotemporal dementia mutant tau promotes aberrant Fyn nanoclustering in hippocampal dendritic spines. *Elife* 8:e45040.
- Patrick GN, Zukerberg L, Nikolic M, de la Monte S, Dikkes P, Tsai LH (1999) Conversion of p35 to p25 deregulates Cdk5 activity and promotes neurodegeneration. *Nature* 402:615–622.
- Prybylowski K, Chang K, Sans N, Kan L, Vicini S, Wenthold RJ (2005) The synaptic localization of NR2B-containing NMDA receptors is controlled by interactions with PDZ proteins and AP-2. *Neuron* 47:845–857.
- Qian W, Liu F (2014) Regulation of alternative splicing of tau exon 10. *Neurosci Bull* 30:367–377.
- Regan P, Whitcomb DJ, Cho K (2017) Physiological and pathophysiological implications of synaptic tau. *Neuroscientist* 23:137–151.
- Rockenstein E, Overk CR, Ubhi K, Mante M, Patrick C, Adame A, Bisquert A, Trejo-Morales M, Spencer B, Masliah E (2015) A novel triple repeat mutant tau transgenic model that mimics aspects of Pick's disease and fronto-temporal tauopathies. *PLoS One* 10:e0121570.
- Sanford AM (2018) Lewy body dementia. *Clin Geriatr Med* 34:603–615.
- Singh B, et al. (2019) Tau is required for progressive synaptic and memory deficits in a transgenic mouse model of α -synucleinopathy. *Acta Neuropathol* 138:551–574.
- Su KH, Cao J, Tang Z, Dai S, He Y, Sampson SB, Benjamin IJ, Dai C (2016) HSF1 critically attunes proteotoxic stress sensing by mTORC1 to combat stress and promote growth. *Nat Cell Biol* 18:527–539.
- Teravskis PJ, et al. (2018) A53T mutant alpha-synuclein induces tau-dependent postsynaptic impairment independently of neurodegenerative changes. *J Neurosci* 38:9754–9767.
- Teravskis PJ, Ashe KH, Liao D (2020) The accumulation of tau in postsynaptic structures: a common feature in multiple neurodegenerative diseases? *Neuroscientist* 26:503–520.
- Teravskis PJ, Oxnard BR, Miller EC, Kemper L, Ashe KH, Liao D (2021) Phosphorylation in two discrete tau domains regulates a stepwise process leading to postsynaptic dysfunction. *J Physiol* 599:2483–2498.
- Terry RD, Masliah E, Salmon DP, Butters N, DeTeresa R, Hill R, Hansen LA, Katzman R (1991) Physical basis of cognitive alterations in Alzheimer's disease: synapse loss is the major correlate of cognitive impairment. *Ann Neurol* 30:572–580.
- Tracy TE, Gan L (2018) Tau-mediated synaptic and neuronal dysfunction in neurodegenerative disease. *Curr Opin Neurobiol* 51:134–138.
- Uchiyama T, Tsuchiya K (2008) Neuropathology of Pick body disease. *Handb Clin Neurol* 89:415–430.
- Um JW, Nygaard HB, Heiss JK, Kostylev MA, Stagi M, Vortmeyer A, Wisniewski T, Gunther EC, Strittmatter SM (2012) Alzheimer amyloid- β oligomer bound to postsynaptic prion protein activates Fyn to impair neurons. *Nat Neurosci* 15:1227–1235.
- van Swieten JC, et al. (1999) Phenotypic variation in hereditary frontotemporal dementia with tau mutations. *Ann Neurol* 46:617–626.
- Vieira RT, Caixeta L, Machado S, Silva AC, Nardi AE, Arias-Carrion O, Carta MG (2013) Epidemiology of early-onset dementia: a review of the literature. *Clin Pract Epidemiol Ment Health* 9:88–95.
- Wesseling H, et al. (2020) Tau PTM profiles identify patient heterogeneity and stages of Alzheimer's disease. *Cell* 183:1699–1713.
- Wiens KM, Lin H, Liao D (2005) Rac1 induces the clustering of AMPA receptors during spinogenesis. *J Neurosci* 25:10627–10636.
- Wszolek ZK, Tsuboi Y, Ghetti B, Pickering-Brown S, Baba Y, Cheshire WP (2006) Frontotemporal dementia and parkinsonism linked to chromosome 17 (FTDP-17). *Orphanet J Rare Dis* 1:30.
- Xia D, Li C, Götz J (2015) Pseudophosphorylation of tau at distinct epitopes or the presence of the P301L mutation targets the microtubule-associated protein tau to dendritic spines. *Biochim Biophys Acta* 1852:913–924.
- Yamaoka LH, et al. (1996) Linkage of frontotemporal dementia to chromosome 17: clinical and neuropathological characterization of phenotype. *Am J Hum Genet* 59:1306–1312.
- Zheng N, Jeyifous O, Munro C, Montgomery JM, Green WN (2015) Synaptic activity regulates AMPA receptor trafficking through different recycling pathways. *Elife* 4:e06878.